การควบคุมแบบสัมพรรคเป็นช่วงสำหรับจักรยานอัตตาณัติโดยใช้ผลของไจโรสโคป

นาย สมพล สุนทระศานติก

วิทยานิพนธ์นี้เป็นส่วนหนึ่งของการศึกษาตามหลักสูตรปริญญาวิศวกรรมศาสตรมหาบัณฑิต
สาขาวิชาวิศวกรรมไฟฟ้า ภาควิชาวิศวกรรมไฟฟ้า
คณะวิศวกรรมศาสตร์ จุฬาลงกรณ์มหาวิทยาลัย
ปีการศึกษา 2553

PIECEWISE AFFINE CONTROL FOR AUTONOMOUS BICYCLE
USING GYROSCOPIC EFFECT

Mr. Sompol Suntharasantic

A Thesis Submitted in Partial Fulfillment of the Requirements
for the Degree of Master of Engineering Program in Electrical Engineering
Department of Electrical Engineering
Faculty of Engineering
Chulalongkorn University
Academic Year 2010

Thesis Title	PIECEWISE AFFINE CONTROL FOR AUTONOMOUS BICYCLE USING GYROSCOPIC EFFECT
By	Mr. Sompol Suntharasantic
Field of Study	Electrical Engineering
Thesis Advisor	Assistant Professor Manop Wongsaisuwan, Ph.D.

Accepted by the Faculty of Engineering, Chulalongkorn University in Partial Fulfillment of the Requirements for the Master's Degree

.... Dean of the Faculty of Engineering
(Associate Professor Boonsom Lerdhirunwong, Dr. Ing.)

THESIS COMMITTEE

.... Chairman
(Associate Professor David Banjerdpongchai, Ph.D.)

.... Thesis Advisor
(Assistant Professor Manop Wongsaisuwan, Ph.D.)

.... External Examiner
(Associate Professor Waree Kongprawechnon, Ph.D.)

สมพล สุนทระศานติก : การควบคุมแบบสัมพรรคเป็นช่วงสำหรับจักรยานอัตตาณัติโดยใช้ผลของไจโรสโคป (PIECEWISE AFFINE CONTROL FOR AUTONOMOUS BICYCLE USING GYROSCOPIC EFFECT) อ. ที่ปรึกษาวิทยานิพนธ์หลัก : ผศ. ดร. มานพ วงศ์สายสุวรรณ, 64 หน้า

วิทยานิพนธ์ฉบับนี้นำเสนอแนวคิดใหม่ในการควบคุมจักรยานอัตตาณัติโดยใช้ผลของไจโรสโคปด้วยวิธีการควบคุมแบบสัมพรรคเป็นช่วง เราพิจารณาระบบจักรยานอัตตาณัติที่ไม่มีเสถียรภาพโดยธรรมชาติที่ความเร็วไปข้างหน้าและความเร็วในการหมุนคงที่ จักรยานประกอบติดกับจานหมุนไจโรสโคปที่ใช้เป็นตัวขับดันสำหรับสร้างเสถียรภาพให้กับมุมล้มของจักรยาน ตัวแปรต่าง ๆ ในระบบวัดมาจากตัวจักรยานขนาดผู้ใหญ่และบางตัวแปรหาได้โดยอ้อมจากโปรแกรมช่วยออกแบบด้วยคอมพิวเตอร์ แบบจำลองไม่เชิงเส้นของระบบจักรยานถูกประมาณด้วยชุดของแบบจำลองเชิงเส้นหรือแบบจำลองสัมพรรคเป็นช่วงซึ่งทำให้ค่าผิดพลาดของแบบจำลองมีค่าลดลงแม้กระทั่งอยู่นอกย่านการทำงานก็ตาม เพื่อที่จะสร้างเสถียรภาพให้กับระบบไม่เชิงเส้นนี้ เราใช้แบบจำลองสัมพรรคเป็นช่วงในการออกแบบตัวควบคุมป้อนกลับ ปัญหาการสังเคราะห์ตัวควบคุมได้เปลี่ยนให้เป็นปัญหาอสมการเมทริกซ์เชิงเส้น อัตราขยายป้อนกลับที่เป็นไปได้หาได้โดยอาศัยฟังก์ชันเลียปูนอฟกำลังสองครอบคลุมเป็นพื้นฐานเพื่อรับประกันเสถียรภาพสำหรับทุกย่าน ผลการจำลองยืนยันประสิทธิผลของวิธีการนี้

ภาควิชา ....วิศวกรรมไฟฟ้า.... ลายมือชื่อนิสิต ....[signature]....
สาขาวิชา ....วิศวกรรมไฟฟ้า.... ลายมือชื่อ อ.ที่ปรึกษาวิทยานิพนธ์หลัก ....[signature]....
ปีการศึกษา ....2553....

5270700721 : MAJOR ELECTRICAL ENGINEERING

KEYWORDS : BICYCLE ROBOT / GYROSCOPIC STABILIZATION / PIECEWISE AFFINE SYSTEM / SINGLE TRACK VEHICLE / LINEAR MATRIX INEQUALITIES

SOMPOL SUNTHARASANTIC : PIECEWISE AFFINE CONTROL FOR AUTONOMOUS BICYCLE USING GYROSCOPIC EFFECT. ADVISOR : ASST. PROF. MANOP WONGSAISUWAN, Ph.D., 64 pp.

This thesis proposes the new idea of autonomous bicycle control using gyroscopic effect by piecewise affine control method. We considers the naturally unstable autonomous bicycle system at constant forward and rotational speeds. The bicycle is attached with a gyroscopic flywheel acting as an actuator for roll angle stabilization. The system parameters are measured from the adult size bicycle body and some parameters are obtained indirectly from CAD program. The nonlinear model of the bicycle system is approximated by a set of linear model or piecewise affine models which minimizes the model error even outside the operating regions. To stabilize this nonlinear system, we use the piecewise affine model to design the feedback controller. The controller synthesis problem is cast as a Linear Matrix Inequalities problem. The feasible feedback control gain is derived based on a globally quadratic Lyapunov function to guarantee the system stability for all regions. The simulation confirms the effectiveness of this approach.

Department Electrical Engineering
Field of Study Electrical Engineering
Academic Year 2010

Student's Signature สมพล สุนทรศานติ์
Advisor's Signature มานพ วงศ์สายสุวรรณ

Acknowledgments

I would like to express my profound gratitude to my principal advisor, Assistant Professor Manop Wongsaisuwan, for his kind guidance, helpful advice, and constructive suggestions on the piecewise affine control used in my research.

I would like to thank to all the committee members of my research. Associate Professor David Banjerdpongchai who provides me with the necessary background on control system theory and kindly served on the thesis committee as a chairman. I am also grateful to Dr. Waree Kongprawechnon for her intutive questions and comments which help me a lot for the improvement in the research.

I gratefully acknowledge the Scholarship from Electrical Engineering Department for the financial support throughout my Master's Degree study. Many thanks to colleague, Prachya Rungtweesuk, a Bachelor's student who was hard-working and made a well support in technical problem while this research was ongoing. In particular, I would like to thank to the people who works hard on the optimization software running on MATLAB "YALMIP" toolbox package, the solver "SDPT3" for efficiently solving the formulations. Also, the prior CSRL members who created and developed the LaTeX Class for this Thesis.

Finally, I would like to thank my family for their understanding and support during my study. Thanks are also given to all members of Control Systems Research Laboratory, Chulalongkorn University for their encouragement and friendship.

Contents

Figure Page

List of Tables

Table Page

List of Figures

Figure Page

Figure Page

CHAPTER I

INTRODUCTION

1.1 Research Motivation

A bicycle was first introduced in the 19th century [1] and still popular over the world up to now. The bicycle has attractive performances. It has light-weight, narrow body, ability to travel to a steeper and rough terrain with also lower installation and maintenance costs. In the environment-friendly aspect, bicycles produce low noise pollution and no CO_2 emission from the organic fuel. Various types of bicycles have been conventionally manufactured without consideration on their dynamics. However, as the advent and evolution of the computer and electronic sensors, the complex control system becomes more feasible.

Bicycle researches induce a rich problem in the area of mechanics (modeling technique) and nonlinear control (control technique). Moreover, the method to control the bicycle can be divided by taking the actuator type into account. For example, it is obvious to see how we control the bicycle by steering the handlebar and balancing our bodies. Another method which cannot be realized by a human rider is to use the flywheel with high spinning rate and precessing about another perpendicular axis. By exploiting the gyroscopic effect, the flywheel generates the torque to help stabilize the bicycle. Since the technique is possible both when the bicycle stands at zero-speed and on moving, we decide to tackle this bicycle control problem with this type of actuator.

The derivation of the bicycle control has 2 main approaches which are the Newtonian approach (Force/Torque balance) and the Lagrangian approach (Conservation of Energy). We have selected the model that mostly fits our aim of research. Our model is from Spry and Girard (2008) [2] which is mainly concerning the model derivation and verification. This model describes the dynamics of bicycle at a constant forward and rotating speed of the bicycle with gyroscopic flywheel and was derived through the Lagrangian method. For our research, the parameter size is on the larger scale comparing with the experiment in [2]. Our parameters are based on the human size bicycle, not a toy size as presented in [2]. The proposed control method was a simple selection of the appropriate gain to satisfy the stability condition of the linearized model. This motivates our research to develop the nonlinear control algorithm for this model.

The bicycle with gyroscopic flywheel model is in fact nonlinear and usually linearized about its operating point to make it possible for using linear control method. To our knowledge, there is no effective result on the nonlinear control of this model type. Therefore, it is an advantage to extend the operating range of bicycle rolling angle while keeping less model error as much as possible by using the new method based on linear models. This results in our proposed control method, the Piecewise Affine (PWA) Control.

PWA systems belongs to the promising class of representation of nonlinear systems by approximating the nonlinearity with linear or affine functions. It can be considered as a natural model class for nonlinear systems since it has been used to represent a range of nonlinearities such as dead zones, saturations, and hysteresis with arbitrary accuracy. Our research will focus on approximating the nonlinear model to PWA model and deriving the control law based on Piecewise Quadratic (PWQ) criteria. We mainly refer the theory of PWA control to the results in [3].

1.2 Literature Review

The structure of the literature review will be presented in 2 parts: the bicycle part and the PWA control part.

Many researches on the bicycle dynamics model and stability analysis and control were done since the late of 19th century. Many papers discussed about the analysis of bicycle with rider control qualitatively. Some did the analysis with a bunch of equations to study its dynamics. The nearly perfect review of bicycle model history was done by A. Schwab *et al.* [4].

Various types of the bicycle model were presented along the century. Every type is concerning with the rolling angle or leaning angle because we are talking about the stability of the upright standing bicycle. Human exploits the advantage of a steering handlebar and body leaning himself to control the path and stabilize the rolling angle. Most of researchers present the interaction between rolling angle and steering angle and use the rolling angle to act like a feedback controller for stabilizing the bicycle. N. Getz presented the nonlinear dynamic model with steering and forward velocity input [5], [6], [7], [8]. His model was derived by constrained Lagrangian method and improved in [9] with additional issue of non-zero front fork angle. M. Defoort [10] applied sliding-mode control scheme to Getz's model. Other works in [11], [12], [13] neglected the front fork angle. Franke *et al.* derived the equation of motion by Newton's formulation [14]. In 2005, Åström [15] released a good summary of bicycle dynamic and control and also the simple linearized second-order model with derivation. One year later, Limebeer and Sharp [16] wrote the more exhaustive models for bicycles and motorcycles including inside analysis of pneumatic tire deflation, flexible frame, etc. A series of paper from Guo showed the different types of control method to this kind of model; nonlinear stabilization [17], LQR [18], fuzzy sliding-mode [19], DFL nonlinear control [20]. Moreover, it was proved that the bicycle with a positive front-fork can be self-stabilized at a specific interval of speed where the real part of eigenvalues were investigated to stay in the left-half plane [4], [21].

The bicycle robot with balancer control was presented in [22] and also balancer together with steering control [23], [24] to enlarge the region of stability. This type of model is not widely investigated as well as the gyroscopic stabilization [2], [25], [26], [27], [28]. Parnichkun (2008) [25] applied the particle-swarm optimization to the proposed model from Gallaspy (1999) [27]. This model captures the bicycle dynamics at the zero forward velocity. The model in [28] incorporated the forward moving velocity but lacked of simulation to verify the model validation. The recent gyroscopic stabilization from [2] is more reliable since it is presented with the clear derivation and model validation by both simulation and real hardware implementation. It included the forward moving velocity and rotating velocity, and left the higher-level study in control part for further development.

The guideline for bicycle project and hardware design can be found in Michini (2006) [29] and a very completed instructive hardware project report “Experimental Validation of a Model for the Motion of an Uncontrolled Bicycle” by Kooijman (2006) [30].

The Piecewise Affine Control or sometimes called Piecewise Linear Control are presented as a kind of hybrid system and the model is varied according to the region which the state is staying. The circuit theory community was said to be the first who recognized PWA systems as an interesting system class [3]. At the beginning, the research on PWA systems considered the model representation [31], [32], especially on the electric network [33]. Model approximation of Nonlinear system by linear model in each region is still be an interesting problem as well. This problem tends to be more complicated when the number of partitioned states is increasing and also more constraints are added to made the smooth continuity at the boundary. The research on PWA model approximation can be found in [34], [35], [36]. To guarantee the stability of the PWA systems, the studies on finding the Quadratic Lyapunov function were proposed by Hassibi and Boyd [37]. This stability problem was also covered the hybrid system and solved via LMIs approach [38]. The PWA optimal control can be found in [39]. The summarize of Piecewise Linear Control was done by Johansson [3]. Besides, one interesting branch of research on PWA is PWA Identification which can be found in [40], [41], [42].

The applications of PWA control are continue to release: Anti-Wind up controller [43], PWA control of a boiler-turbine unit [44], MPC [45], etc. There is not much papers published about PWA applying with vehicle dynamics control application. However, we have found some application to a vehicle yaw control in [46], [47].

This thesis mainly follows the PWA system theory presented extensively in [3].

1.3 Thesis Objective

The main objective of this research is to design a piecewise affine controller based on piecewise quadratic stability criteria for the autonomous bicycle with gyroscopic flywheel stabilization and to build a start-up prototype bicycle for the future implementation work on the bicycle robot. We first obtain the bicycle dynamics model from the previous work and then approximate the nonlinear model into the form of a piecewise affine model. The controller based on a global piecewise quadratic Lyapunov function is derived by solving the semidefinite programming problem.

1.4 Scope of Thesis

1. To derive Piecewise affine bicycle with gyroscopic flywheel model
2. To design the feedback controller based on the Piecewise Quadratic criteria
3. To build a physical prototype of the bicycle robot for retrieving the practical bicycle parameters and for a future research

1.5 Methodology

1. Literature review on Bicycle model and PWA systems.
2. Select an autonomous bicycle robot model with gyroscopic stabilization.
3. Do parameter measurement from the real bicycle.
4. Derive the PWA model from the selected nonlinear dynamics bicycle model.
5. Design the Piecewise Quadratic controller for PWA bicycle model.

1.6 Contributions

1. A Piecewise Affine bicycle with gyroscopic flywheel model.
2. A Piecewise Affine controller for bicycle with gyroscopic flywheel.
3. A start-up prototype of experimental bicycle with gyroscopic flywheel.

1.7 Structure of Thesis

The organization of the thesis is as follows. In the next chapter, the related theories, which are the primary knowledge and some are considered to be in bicycle robot environment, are presented. Chapter 3 presents Experimental Bicycle. Chapter 4 presents the bicycle dynamic model. Chapter 5 presents PWA model for the bicycle robot. Chapter 6 presents piecewise affine control for bicycle robot. In the last chapter, conclusions are given.

CHAPTER II

RELATED THEORIES

In this chapter, an overview of the fundamental theory used in modeling and designing PWA control systems is given.

2.1 Bicycle Properties

In this section, we describe the important properties of the bicycle that affect the stability of the bicycle.

2.1.1 Nature of the Bicycle

The bicycle is naturally unstable. When it stays upright, by no holding force, it will roll down left or right. However, it is not too hard to learn riding a bicycle by human. We turn the steering to the right when the bicycle seems to roll to the right side. It behaves the same manner for the left hand side. That is a mean of dynamic control of the bicycle.

2.1.2 The Trail

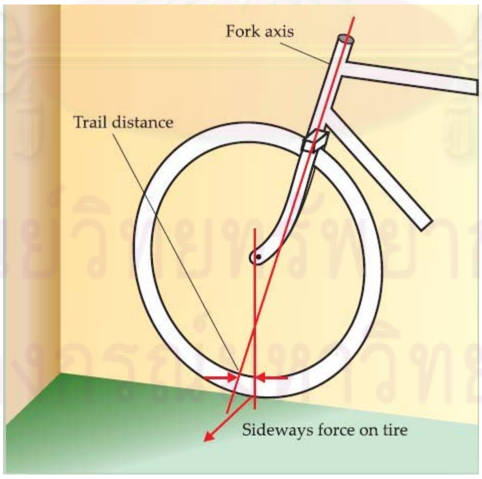

Figure 2.1: The position of the trail distance of the bicycle [48].

At the beginning, the bicycle has no trail or front fork. That means the handle bar axis is perpendicular to the ground. This type of bicycle has no effect of trail to the rolling angle when we steer the handlebar. The non-zero trail distance produce a major impact to the dynamics of the bicycle. D.E.H. Jones [48] studied this effect by constructing the bicycle with different kinds of trail distance. The interesting case is the positive trail which we are always familiar with. Positive trail provides a torque about the steering axis that counteracts angular momentum when the bike body leans to the left or the right. This counteracting torque causes the front wheel to turn in the direction opposite to the direction of lean, and thus enhances the stability of the bike. This torque does not appear only when the bicycle is moving but it is also generated when the bicycle is tilting.

2.1.3 Self-stability

Imagine when the bicycle is running forward along a road with non-zero speed and no maneuvering. We know that the bicycle is an unstable system. However, it was proved that the bicycle that has the positive front fork trail is itself stable in an interval of speed [15, 16, 21]. David E.H. Jones [48] emphasized that the steering geometry dramatically influences the stability. When the bicycle is tilting, its center of gravity is lower. Then, the front wheel steers to the tilting direction to minimize its gravitational potential energy. This will not occur if the trail is zero. In addition, Åström presented in another perspective. The ground reaction force exerts a torque on the front fork assembly to made the front fork steer. The analysis through the simple second order linearized model is discussed in [15].

It is essential to understand the self-stabilization behavior of the bicycle. To control the bicycle upright and running on a straight path, we do not need any inputs to stabilize the bicycle in a particular speed range unless we have a curvature path. Here, we show our analysis using the experimental bicycle parameters that we measure ourselves. The moment of inertias are retrieved via CATIA CAD-software. The analysis is based on the linear 4th-order equation (The Whipple model) in [21]. The equation of motion is

$$\mathbf{M}\begin{bmatrix}\ddot{\varphi}\\ \ddot{\beta}\end{bmatrix} + v\mathbf{C_1}\begin{bmatrix}\dot{\varphi}\\ \dot{\beta}\end{bmatrix} + (g\mathbf{K_0} + v^2\mathbf{K_2})\begin{bmatrix}\varphi\\ \beta\end{bmatrix} = \begin{bmatrix}T_\varphi\\ T_\beta\end{bmatrix} \tag{2.1}$$

With our real measured and CAD-program calculated parameters in Table 2.1, we have

$$\begin{aligned}\mathbf{M} &= \begin{bmatrix}8.6551 & 0.9466\\ 0.9466 & 0.3165\end{bmatrix} & \mathbf{C_1} &= \begin{bmatrix}0 & 9.3019\\ -0.7057 & 1.4885\end{bmatrix}\\ \mathbf{K_0} &= \begin{bmatrix}-14.7837 & -2.0400\\ -2.040 & -0.7164\end{bmatrix} & \mathbf{K_2} &= \begin{bmatrix}0 & 14.0139\\ 0 & 1.9743\end{bmatrix}\end{aligned} \tag{2.2}$$

The result is that the self-stable speed range is $3.60 < v < 10.26$ m/s. Note that the range is wider than a bicycle with the rider which has more weight.

We will take this advantage of self-stability to leave the steering bar move freely when we want the bicycle to run on a straight path at that particular speed range. Also, it is not necessary to control the roll angle by precessing the gyroscopic flywheel when the bicycle is self-stabilized. The explanation about how to control the bicycle roll angle will be discuss in the section 4.

2.1.4 Gyroscopic Effect at the Front Wheel

The gyroscopic action at the front wheel affect the stability of the bicycle. In Figure 2.3, we assume the bicycle is running with forward speed. According to our earth fixed coordinate frame, the spinning axis is perpendicular to the direction of the bicycle and have a positive ω_{speed}. To say, it points to the same direction as y-axis. Next, when we steer the handlebar to the left, ω_{steer} vector points vertically with the z-axis. This will result to the bicycle to roll to the right side. The rolling direction can be found mathematically by $\tau_{\text{roll}} = (I_{s2}\omega_{\text{speed}}\mathbf{e}_2) \times \omega_{\text{steer}}\mathbf{e}_3 = \omega_{\text{roll}}\mathbf{e}_1$ where I_{s2} is the moment of inertia of the steering handlebar with respect to the principal axis $\mathbf{e}_2$.

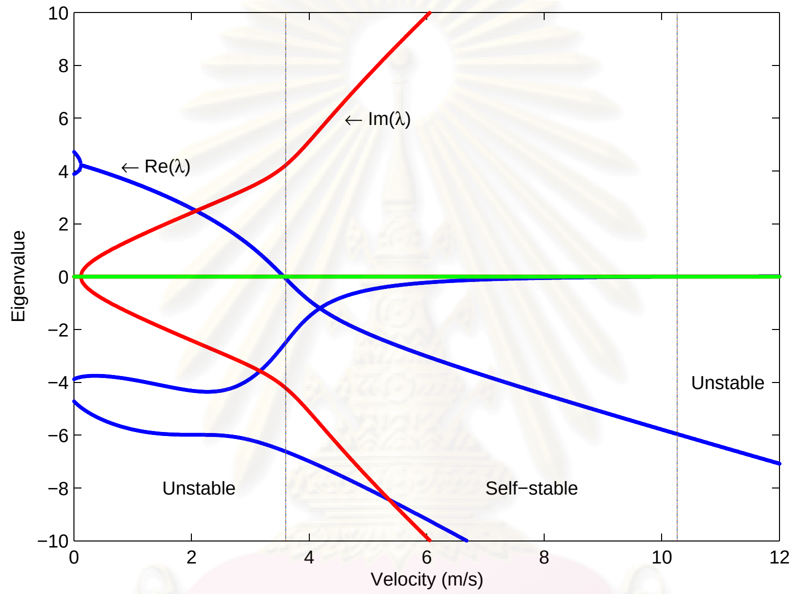

Figure 2.2: Eigenvalues from the linearized self-stability analysis.

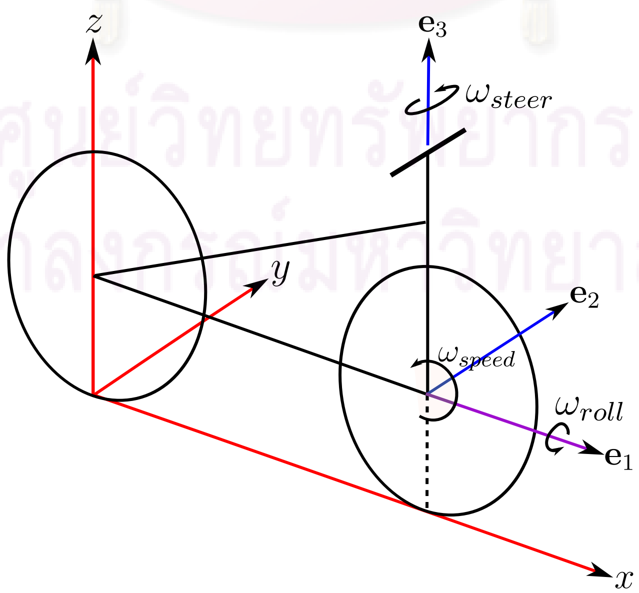

Figure 2.3: Gyroscopic effect at the front wheel coordinate and notation.

Table 2.1: Parameters of the Experimental Bicycle for Self-stability Analysis.

Parameter	**Symbol**	**Value**	**Unit**
Wheelbase	w	1.07	m
Trail	c	0.12	m
Front fork angle	λ	20.56	degree
Front wheel			
Mass	m_F	2.234	kg
Mass center	(x_F, y_F, z_F)	(1.07,0,0.32)	m
Radius	r_F	0.32	m
Moment of inertia	$\begin{bmatrix} I_{Fxx} & I_{Fxy} & I_{Fxz} \\ I_{Fyx} & I_{Fyy} & I_{Fyz} \\ I_{Fzx} & I_{Fzy} & I_{Fzz} \end{bmatrix}$	$\begin{bmatrix} 0.099 & 0 & 0 \\ 0 & 0.197 & 0 \\ 0 & 0 & 0.099 \end{bmatrix}$	kg· m^2
Rear wheel			
Mass	m_R	2.234	kg
Mass center	(x_R, y_R, z_R)	(0,0,0.32)	m
Radius	r_R	0.32	m
Moment of inertia	$\begin{bmatrix} I_{Rxx} & I_{Rxy} & I_{Rxz} \\ I_{Ryx} & I_{Ryy} & I_{Ryz} \\ I_{Rzx} & I_{Rzy} & I_{Rzz} \end{bmatrix}$	$\begin{bmatrix} 0.099 & 0 & 0 \\ 0 & 0.197 & 0 \\ 0 & 0 & 0.099 \end{bmatrix}$	kg· m^2
Body (with battery)			
Mass	m_B	30	kg
Mass center	(x_B, y_B, z_B)	(0.49,0,0.39)	m
Moment of inertia	$\begin{bmatrix} I_{Bxx} & I_{Bxy} & I_{Bxz} \\ I_{Byx} & I_{Byy} & I_{Byz} \\ I_{Bzx} & I_{Bzy} & I_{Bzz} \end{bmatrix}$	$\begin{bmatrix} 1.995 & 0 & -0.053 \\ 0 & 2.347 & 0 \\ -0.053 & 0 & 0.487 \end{bmatrix}$	kg· m^2
Front fork & Handlebar			
Mass	m_H	2.148	kg
Mass center	(x_H, y_H, z_H)	(0.92,0,0.77)	m
Moment of inertia	$\begin{bmatrix} I_{Hxx} & I_{Hxy} & I_{Hxz} \\ I_{Hyx} & I_{Hyy} & I_{Hyz} \\ I_{Hzx} & I_{Hzy} & I_{Hzz} \end{bmatrix}$	$\begin{bmatrix} 0.168 & 0 & 0.023 \\ 0 & 0.132 & 0 \\ 0.023 & 0 & 0.047 \end{bmatrix}$	kg· m^2
Gyroscopic Flywheel			
Mass	m_G	9.0329	kg
Mass center	(x_G, y_G, z_G)	(0.49,0,0.88)	m
Moment of inertia	$\begin{bmatrix} I_{Gxx} & I_{Gxy} & I_{Gxz} \\ I_{Gyx} & I_{Gyy} & I_{Gyz} \\ I_{Gzx} & I_{Gzy} & I_{Gzz} \end{bmatrix}$	$\begin{bmatrix} 0.138 & 0 & 0 \\ 0 & 0.138 & 0 \\ 0 & 0 & 0.274 \end{bmatrix}$	kg· m^2

Nevertheless, the effect on the bicycle is very small compared to the gravitational torque and gyroscopic flywheel unless the wheel spinning speed is very high. Our model therefore neglects this effect.

2.2 Lagrangian Mechanics

Lagrangian mechanics is a re-formulation of classical mechanics that combines conservation of momentum with conservation of energy [49]. The Lagrangian is an efficient method to derive the equation of motion through the energy aspect. The Lagrangian function $\mathcal{L}$ is defined as

$$\mathcal{L}(q, \dot{q}) \equiv T(q, \dot{q}) - V(q)$$

where T is the Kinetic energy, V is the Potential energy, and q is the generalized coordinate. According to the derivation in [50], the result Lagrangian's equations is then

$$\frac{d}{dt}\left(\frac{\partial \mathcal{L}}{\partial \dot{q}_k}\right) - \frac{\partial \mathcal{L}}{\partial q_k} = Q_k^{(nc)}; \qquad k = 1, 2, \ldots, M \tag{2.3}$$

where Q_k^{nc} is the nonconservative generalized forces.

The Kinetic energy of the rigid body can be calculated by

$$T = \frac{1}{2} m \mathbf{v}_c \cdot \mathbf{v}_c + \frac{1}{2} \mathbf{H}_c \cdot \omega \tag{2.4}$$

or in the matrix form

$$T = \frac{1}{2} m \mathbf{v}_c^T \mathbf{v}_c + \frac{1}{2} \omega^T \mathbf{I}_c \omega \tag{2.5}$$

where $\mathbf{v}_c$ is the linear velocity of the rigid body, ω is the angular velocity about its mass center, $\mathbf{H}_c$ is the angular momentun about the mass center, and $\mathbf{I}_c$ is the moment of inertia of the rigid body.

The Potential energy may be caused by gravitational force, elastic spring force, elastic force between two charges, etc. It can be represented as

$$\mathbf{F} = -\nabla V(\mathbf{r}) \tag{2.6}$$

In this thesis, the instrumental force for the potential energy is from the gravity near the Earth's surface. It is given by

$$\mathbf{F} = -mg\mathbf{e}_z, \qquad V = mgz$$

2.3 Piecewise Affine System

The Piecewise Affine system is a kind of nonlinear system which is linear in each local cell/partition where each partition has its own dynamics. The fascinating advantage of this type of control is that it is linear, however in a region, but provides more accuracy than a linearized model and the controller synthesis based on Piecewise Quadratic Lyapunov function is global. One time solving a batch LMIs problem, the obtained gain can be used to stabilize the system in overall operating point.

2.3.1 Model Representation

Consider piecewise affine systems on the form

$$\begin{cases} \dot{x}(t) = A_i x(t) + a_i + B_i u(t) \\ y(t) = C_i x(t) + c_i + D_i u(t) \end{cases} \quad x \in X_i, i \in I \tag{2.7}$$

Here, $x(t)$ is the continuous state vector, $u(t)$ is an exogenous signal (control or disturbance, depending on the context), $\{X_i\}_{i \in I} \subseteq \mathbf{R}^n$ is a partition of the state space into a number of closed polyhedral cells and I is the set of cell indices. Assume that the cells have disjoint interior (so that any two cells can only share a common boundary) and that they form a partition of some compact subspace $X = \cup_{i \in I} X_i$ of $\mathbf{R}^n$. Let $x(t)$ be a continuous piecewise function on the time interval $[0, T]$. We say that $x(t)$ is a trajectory of (2.7), if for every $t \in [0, T]$ such that the derivative $\dot{x}(t)$ is defined, the equation $\dot{x}(t) = A_i x(t) + a_i + B_i u(t)$ holds for all i with $x(t) \in X_i$. Note that for a given system there may be initial values such that a corresponding trajectory only exists for small T.

Focus on properties of the equilibrium $x = 0$, and let $I_0 \subseteq I$ be the index set for cells that contain the origin, let $I_1 = I \setminus I_0$, and assume that $a_i = 0$, $c_i = 0$ for $i \in I_0$. For convenient, we use the notation $\bar{x} = \begin{bmatrix} x & 1 \end{bmatrix}^T$,

$$\bar{A}_i = \begin{bmatrix} A_i & a_i \\ 0 & 0 \end{bmatrix}, \ \bar{B}_i = \begin{bmatrix} B_i \\ 0 \end{bmatrix}, \ \bar{C}_i = \begin{bmatrix} C_i & c_i \end{bmatrix}$$

and re-write (2.7) as

$$\begin{aligned} \dot{\bar{x}}(t) &= \bar{A}_i \bar{x}(t) + \bar{B}_i u(t) \\ y(t) &= \bar{C}_i \bar{x}(t) + D_i u(t) \end{aligned} \tag{2.8}$$

Each polyhedral cell of the system (2.8) is partitioned by K hyperplanes

$$\partial \mathcal{H}_k = \{x \,|\, H_k x + h_k = 0\} \qquad \forall h_k \leq 0, \quad k = 1, \ldots, K \tag{2.9}$$

For convenient, all hyperplanes are represented as a *hyperplane matrix*

$$\bar{H} = \begin{bmatrix} H_k & h_k \end{bmatrix} \tag{2.10}$$

The polyhedral cells are represented on the form

$$X_i = \{x \,|\, G_i x + g_i \succeq 0\} \tag{2.11}$$

where $\succeq$ denotes elementwise inequality. To made it more compact, we construct matrices

$$\bar{G}_i = \begin{bmatrix} G_i & g_i \end{bmatrix}$$

where $\bar{G}_i$ is called a *cell identifier*.

2.3.2 Quadratic Stability

The term *quadratic stability* refers to stability that can be established using a quadratic Lyapunov function. It is possible to prove stability of piecewise linear systems using a globally quadratic Lyapunov function $V(x) = x^T P x$. In particular, if $a_i = 0 \; \forall i \in I$ and there exists $P > 0$ such that

$$A_i^T P + P A_i < 0 \qquad\qquad \forall i \in I \tag{2.12}$$

Then every trajectory of (2.7) tends to zero exponentially. The stability of a family of linear system depends on each cell partition. The equation (2.12) are linear matrix inequalities in P which can be solved as a convex optimization problem.

To verify that there exists no matrix P satisfying (2.12), it is a dual problem to find a positive definite matrices R_i , $i \in I$ such that

$$\sum_{i \in I} A_i^T R_i + R_i A_i > 0 \tag{2.13}$$

If the condition (2.13) is satisfied, then the Lyapunov function P in (2.12) will not be admitted.

2.3.3 Piecewise Quadratic Stability

We consider functions that are continuous and piecewise quadratic. This condition must be satisfied with all cell X_i, so it is sufficient to require that

$$x^T(A_i^T P + PA_i)x < 0, \quad \text{for } x \in X_i \tag{2.14}$$

To obtain a relaxed conditions for quadratic stability, one applies the $\mathcal{S}$-procedure and construct positive definite matrices S_i, $i \in I$ such that

$$A_i^T P + PA_i + S_i < 0 \tag{2.15}$$

Matrices S_i in $\mathcal{S}$-procedure can be construct from the system description, in this case are cell bounding matrices E_i and $\bar{E}_i$. With nonnegative entries matrices U_i, we have

$$\begin{array}{ll} x^T E_i^T U_i E_i x \geq 0 \quad , & x \in X_i, i \in I_0 \\ \bar{x}^T \bar{E}_i^T U_i \bar{E}_i \bar{x} \geq 0 \quad , & x \in X_i, i \in I_1 \end{array} \tag{2.16}$$

The cell boundings are important parameters from the partition information to enforce the positivity of the quadratic Lyapunov functions for all $x \in X_i$. The *polyhedral cell bounding* matrices can be defined as

$$\bar{E}_i = \begin{bmatrix} E_i & e_i \end{bmatrix} \quad \text{and} \quad \bar{E}_i \bar{x} \succeq 0, \quad x(t) \in X_i$$

The next step is to make the quadratic Lyapunov functions to be valid in all regions and continuous across cell boundaries. Let

$$\begin{array}{ll} P_i & = F_i^T T F_i, \quad i \in I_0 \\ \bar{P}_i & = \bar{F}_i^T T \bar{F}_i, \quad i \in I_1 \end{array} \tag{2.17}$$

where F_i and $\bar{F}_i$ are called the *continuity matrices* with their properties

$$\bar{F}_i = \begin{bmatrix} F_i & f_i \end{bmatrix} \quad \text{and} \quad \bar{F}_i \bar{x}(t) = \bar{F}_j \bar{x}(t) \quad \text{for } x(t) \in X_i \cap X_j$$

Since the expression for P_i is linear in a symmetric matrix T, it will be possible to state the search for a piecewise quadratic Lyapunov function as a set of linear matrix inequalities. The constructed Lyapunov function will in general have the form

$$V(x) = \begin{cases} x^T P_i x, & x \in X_i, \quad i \in I_0 \\ \bar{x}^T \bar{P}_i \bar{x}, & x \in X_i, \quad i \in I_1 \end{cases} \tag{2.18}$$

Next, we formulate LMIs for finding an existence of piecewise quadratic Lyapunov function of the system (2.7).

Theorem 2.1 (Piecewise Quadratic Stability)**.** *[3]*
Consider symmetrics T, U_i *and* W_i *have nonnegative entries, while* $P_i = F_i^T T F_i, i \in I_0$ *and* $\bar{P}_i = \bar{F}_i^T T \bar{F}_i, i \in I_1$

$$\begin{cases} 0 > A_i^T P_i + P_i A_i + E_i^T U_i E_i \\ 0 < P_i - E_i^T W_i E_i \end{cases} \quad i \in I_0 \tag{2.19}$$

$$\begin{cases} 0 > \bar{A}_i^T \bar{P}_i + \bar{P}_i \bar{A}_i + \bar{E}_i^T U_i \bar{E}_i \\ 0 < \bar{P}_i - \bar{E}_i^T W_i \bar{E}_i \end{cases} \quad i \in I_1 \tag{2.20}$$

then every trajectory $x(t)$ *of (2.7) with* $u \equiv 0$ *for* $t \geq 0$ *tends to zero exponentially.*

2.3.4 Piecewise Quadratic Stabilization of PWA system

This section will show how to obtain the globally linear state feedback that stabilizes a PWA system. This can be cast as a convex optimization problem. Let us consider the state feedback

$$u = -Lx$$

which results in the closed loop system

$$\dot{x}(t) = (A_i - B_i L)x(t) + a_i \qquad x \in X_i \quad i \in I. \tag{2.21}$$

to be asymptotically stable for all region.

For the quadratic stabilization problem, we need to find a gain L that admits a quadratic Lyapunov function $V(x) = x^T P x$. For each cell X_i, we use the ellipsoid cell boundings

$$\|S_i x + s_i\|_2 \leq 1 \qquad \forall x \in X_i \tag{2.22}$$

or

$$1 - (S_i x + s_i)^T (S_i x + s_i) \geq 0 \qquad \forall x \in X_i \tag{2.23}$$

or

$$\begin{bmatrix} x \\ 1 \end{bmatrix}^T \begin{bmatrix} -S_i^T S_i & -S_i^T s_i \\ -s_i^T S_i & 1 - s_i^T s_i \end{bmatrix} \begin{bmatrix} x \\ 1 \end{bmatrix} \geq 0 \qquad \forall x \in X_i \tag{2.24}$$

and the condition in (2.14) to derive the sufficient condition for PWA system stability via $\mathcal{S}$-procedure. Then, the closed-loop system is quadratically stable if we can find a positive definite matrix $P = P^T \geq 0$ and positive scalars $u_i \geq 0$ such that

$$\begin{cases} 0 > (A_i - B_i L)^T P + P(A_i - B_i L) & i \in I_0 \\ 0 > \begin{bmatrix} (A_i - B_i L)^T P + P(A_i - B_i L) & P a_i \\ a_i^T P & 0 \end{bmatrix} + u_i \begin{bmatrix} -S_i^T S_i & -S_i^T s_i \\ -s_i^T S_i & 1 - s_i^T s_i \end{bmatrix} & i \in I_1 \end{cases} \tag{2.25}$$

The above condition is bilinear in L and P and not efficient to be solved, however the problem can be transformed and resulted in Theorem 2.2.

Theorem 2.2 (Quadratic Stabilization). *[3]*
If there exists a positive definite matrix $Q = Q^T > 0$, positive scalars $v_i \geq 0$ and a matrix Y such that

$$\begin{cases} 0 > QA_j^T + A_jQ - Y^TB_j^T - B_jY \\ 0 < \begin{bmatrix} QA_i^T + A_iQ - Y^TB_i^T - B_iY - v_ia_ia_i^T & QS_i^T - v_ia_is_i^T \\ (QS_i^T - v_ia_is_i^T)^T & v_i(I - s_is_i^T) \end{bmatrix} \end{cases} \tag{2.26}$$

where $j \in I_0$ and $i \in I_1$. Then, the feedback $u = -Lx$ with $L = YQ^{-1}$ renders the piecewise linear system exponentially stable.

In this thesis, we will use this criteria to design the PWA state feedback control laws.

CHAPTER III

EXPERIMENTAL BICYCLE

In this chapter, we focus on the parameter measurement of the prototype autonomous bicycle with gyroscopic flywheel. the critical issues are the bicycle dimensions and the gyroscopic flywheel parameters.

3.1 Bicycle

This bicycle is the adult size bicycle and meets the criteria of the BicyRobo Thailand competition. The wheel base length is more than 50 cm, the diameter of each wheel is more than 50 cm, and the tire width is less than 5 cm. We end up with the our used bicycle in Figure 3.1. The body is a rigid frame without suspension.

Figure 3.1: The selected bicycle before modifying.

To design the new features and estimate the parameters from the real world model, we draw the 3D CAD graphic in CATIA[1]. Figure 3.2 shows the 3D CAD of bicycle robot with the actual measured dimension. The pedal, saddle, barrel adjuster and rear deraileur will be removed from this original bike.

The measured bicycle parameters are collected in Table 2.1. Some parameters such as the moment of inertia is needed to calculated indirectly. Here, we let the CATIA software to calculate them all by inputing the mass that we can simply measure it and the type of part material (to figure out the mass density). These data are used for the whole simulation in this project.

[1]CAD software for designing mechanical part.

Figure 3.2: The 3D CAD drawing of the bicycle before modifying.

Figure 3.3: Bicycle robot attached with gyroscopic flywheel.

3.2 Gyroscopic Flywheel

The flywheel is treated as an actuator for controlling the bicycle rolling angle. We consider the critical case that this actuator can generate the moment to resist the moment produced by the gravitational torque when the bicycle is tilting. While the bicycle rolling angle is larger, the gravitational moment becomes larger too.

From Figure 3.4, $\mathbf{xyz}$ is the global axes and $\mathbf{e}_1\mathbf{e}_2\mathbf{e}_3$ is the principal axes of the flywheel. The basis vector $\{\mathbf{e}_1, \mathbf{e}_2, \mathbf{e}_3\}$ rotate together with the gyroscopic flywheel at the angular velocity $\omega_\mathbf{e}$.

$$\omega_\mathbf{e} = \dot{\varphi}\mathbf{e}_1 + \dot{\alpha}\mathbf{e}_2 \tag{3.1}$$

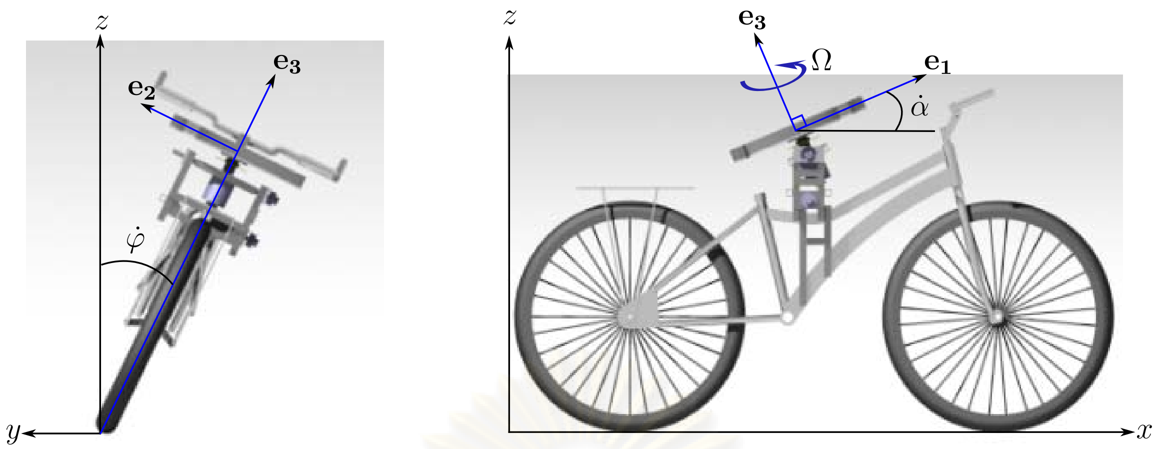

Figure 3.4: The bicycle configuration for sizing the flywheel (mass and dimension).

Let the bicycle initially stands at the rolling angle of φ radian with zero forward moving velocity and the flywheel spin at a constant speed Ω rad/s about $\mathbf{e}_3$-axis and precessing at $\dot{\alpha}$ rad/s about $\mathbf{e}_2$ axis. The angular momentum of the flywheel about O can be written as

$$\mathbf{H}_o = I_{1o}\dot{\varphi}\mathbf{e}_1 + I_{2o}\dot{\alpha}\mathbf{e}_2 + I_{3o}\Omega\mathbf{e}_3 \tag{3.2}$$

where I_{1o}, I_{2o}, I_{3o} are the moment of intertia with respect to the point O. We assign the point O to be the midpoint between the ground contact point of front and rear wheel. The vertical principal $\mathbf{e}_3$-axis of of the flywheel pass through this point. In our case $\dot{\varphi} = 0$ because we assume that the gravitational moment is equal to the moment generated by the precession torque from the gyroscopic effect. By the way, we should note that the flywheel will precess to generate the moment with magnitude greater than the gravitational torque to pull the bicycle back to stand upright at $\varphi = 0$ rad. Yet, we calculate the least moment that the flywheel must be able to generate. Thus, it reduces to

$$\mathbf{H}_o = I_2\dot{\alpha}\mathbf{e}_{2o} + I_{3o}\Omega\mathbf{e}_3 \tag{3.3}$$

Carrying out the details for the change of $\mathbf{H}_o$, we write

$$\begin{aligned}\dot{\mathbf{H}}_o &= I_{2o}\ddot{\alpha}\mathbf{e}_2 + I_{2o}\dot{\alpha}\dot{\mathbf{e}}_2 + I_{3o}\Omega\mathbf{e}_3 + I_{3o}\Omega\dot{\mathbf{e}}_3 \\ &= I_{2o}\ddot{\alpha}\mathbf{e}_2 + I_{2o}\dot{\alpha}(\omega_\mathbf{e}\times\mathbf{e}_2) + I_{3o}\Omega\mathbf{e}_3 + I_{3o}\Omega(\omega_\mathbf{e}\times\mathbf{e}_3) \\ &= I_{3o}\Omega\dot{\alpha}\mathbf{e}_1 + (I_{2o}\ddot{\alpha} - I_{3o}\Omega\dot{\varphi})\mathbf{e}_2 + I_{2o}\dot{\alpha}\dot{\varphi}\mathbf{e}_3\end{aligned}$$

Take $\dot{\varphi} = 0$, we have

$$\dot{\mathbf{H}}_o = I_{3o}\Omega\dot{\alpha}\mathbf{e}_1 + I_{2o}\ddot{\alpha}\mathbf{e}_2 \tag{3.4}$$

This change in $\mathbf{H}_{o1}$ must equal to the gravitational moment $\mathbf{M}_{o1}$ around x-axis. The produced moment is given by

$$\begin{aligned}\mathbf{M}_{o1} &= z_B\mathbf{e}_3\times(-m_Bg\mathbf{k}) + z_G\mathbf{e}_3\times(-m_Gg\mathbf{k}) \\ &= (m_Bz_B + m_Gz_G)g\sin\varphi\mathbf{e}_1\end{aligned} \tag{3.5}$$

From the Euler's equation for rigid-body dynamics $\mathbf{M}_{o1} = \dot{\mathbf{H}}_{o1}$, (3.4), and (3.5), we have

$$I_{3o}\Omega\dot{\alpha} = (m_Bz_B + m_Gz_G)g\sin\varphi \tag{3.6}$$

$$I_{2o}\ddot{\alpha} - I_{3o}\Omega\dot{\varphi} = 0 \tag{3.7}$$

Torque component $\mathbf{e}_2$ of $\dot{\mathbf{H}}_o$ will result at the ground contact point of front and rear wheel and it is resisted by the reaction torque of the ground contact. Therefore, there is no rotational motion for this axis (The bicycle does not tip over to the front or back). The important role to stabilize the bicycle is at the $\mathbf{e}_1$ axis. Its relationship is shown in (3.6). We need an excessive moment to pull the bicycle in the reverse direction. The gyroscopic flywheel should be designed in order to satisfy the equation below

$$(m_B z_B + m_G z_G) g \sin\varphi < I_{3o}\Omega\dot{\alpha} \tag{3.8}$$

Note that $I_{3o} = I_3$ where I_3 is the moment of inertia of the flywheel about its principal axis. For simplicity to manage the calculation, we introduce

$$M_{req} = (m_B z_B + m_G z_G) g \sin\varphi \tag{3.9}$$

$$M_{gen} = I_{3G}\Omega\dot{\alpha} \tag{3.10}$$

Take the parameter value in Table 3.1 and the formula in Table 3.2 to find M_{req} and M_{gen}, we finally get $M_{\text{req}} = 20.5481$ kg·m and $M_{\text{gen}} = 29.8311$ kg·m. The DIY[2] Gyroscopic Flywheel can produce the moment in which its magnitude is greater than the required value with the factor of 1.4518.

Table 3.1: Parameters for Gyroscopic Flywheel Design Calculation.

Parameter	**Symbol**	**Value**	**Unit**
Disk mass	m_d	3.3929	kg
Circular tube mass	m_c	5.6400	kg
Flywheel mass	m_G	9.0329	kg
Bicycle body mass	m_B	30	kg
Outer radius	r_d	0.20	m
Inner radius	r_c	0.18	m
Disk thickness	h_d	0.01	m
Circular tube thickness	h_c	0.03	m
Height of bicycle center of mass	z_B	0.50	m
Height of flywheel center of mass	z_G	1.00	m
Rolling angle	φ	5	degree
Spinning angular velocity	Ω	3000	rpm
Precessing angular velocity	$\dot{\alpha}$	20	degree/s
Gravitational acceleration	g	9.81	m/s^2
Iron mass density	ρ_{Fe}	7874	kg/m^3
Aluminium mass density	ρ_{Al}	2700	kg/m^3

[2]Do It Yourself

Moment of Inertia of Flywheel

The Flywheel is assigned to spin about $\mathbf{e}_3$ axis and precess about $\mathbf{e}_2$ axis. Figure 3.5 shows the dimension and other description for the calculation of the flywheel moment of inertia. Refer to the "List of moments of inertia" from [51], we obtain the moment of inertia in two parts - Disk and Cylindrical tube about the point D and C. Then, we take them to rotate about O using Parallel axis theorem and combine them together by addition. The summary of the Flywheel moment of inertia is in Table 3.2. The mass calculation here are $m_d = \rho_{Al} V_d$, $m_c = \rho_{Fe} V_c$, and $m_G = m_d + m_c$ where ρ_{Al} is the density of Aluminium and ρ_{Fe} is the density of iron.

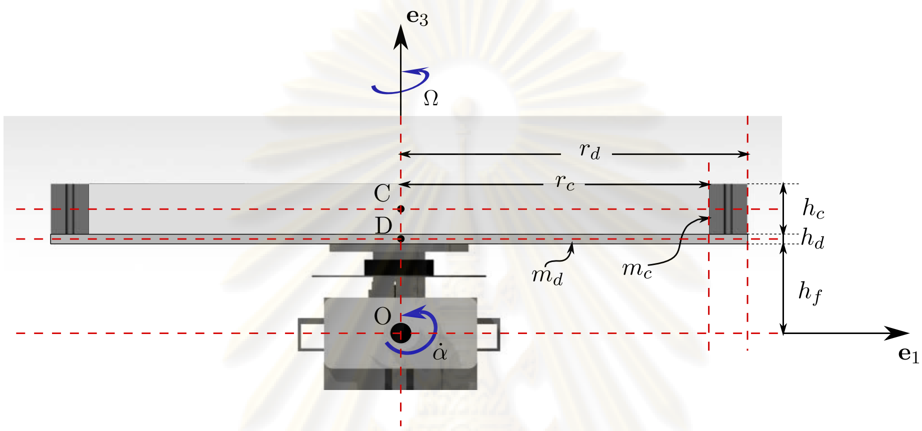

Figure 3.5: Side View Cross-section of Flywheel configuration.

Table 3.2: Summary of Flywheel Moment of Inertia.

Object	I_3	I_2	Volume
Disk (about D)	$I_{3D} = \frac{1}{2} m_d r_d^2$	$I_{2D} = \frac{1}{12} m_d (3r_d^2 + h_d^2)$	$V_D = \pi r_d^2 h_d$
Cylindrical tube (about C)	$I_{3C} = \frac{1}{2} m_c (r_c^2 + r_d^2)$	$I_{2C} = \frac{1}{12} m_c [3(r_c^2 + r_d^2) + h_c^2]$	$V_C = \pi (r_d^2 - r_c^2) h_c$
Gyroscopic Flywheel (about O)	$I_{3G} = I_{3D} + I_{3C}$	$I_{2G} = I_{2D} + m_d h_f^2 + I_{2C} + m_c (h_f + \frac{h_d}{2} + \frac{h_c}{2})^2$	$V_G = V_D + V_C$

CHAPTER IV

BICYCLE DYNAMIC MODEL

The equation of motion of 3D rigid body can be derived in 3 aspects. Those are the conservation of force (torque), momentum (angular momentum), and energy. The model of a bicycle with gyroscopic stabilization is mostly derived by the Lagrangian method (Energy aspect) because it is easy to obtain the linear and angular velocity while the internal force or any other workless forces can be ignored. From the literature review, we have inspected many types and complicated levels of the bicycle. We end up with the nonlinear dynamic model from Spry [2] and extend the model to PWA model.

We next define the bicycle geometry, the assumption and limitation of the model, the notation of the parameters and lastly the nonlinear model with neglecting relatively small-value terms.

4.1 Bicycle Geometry

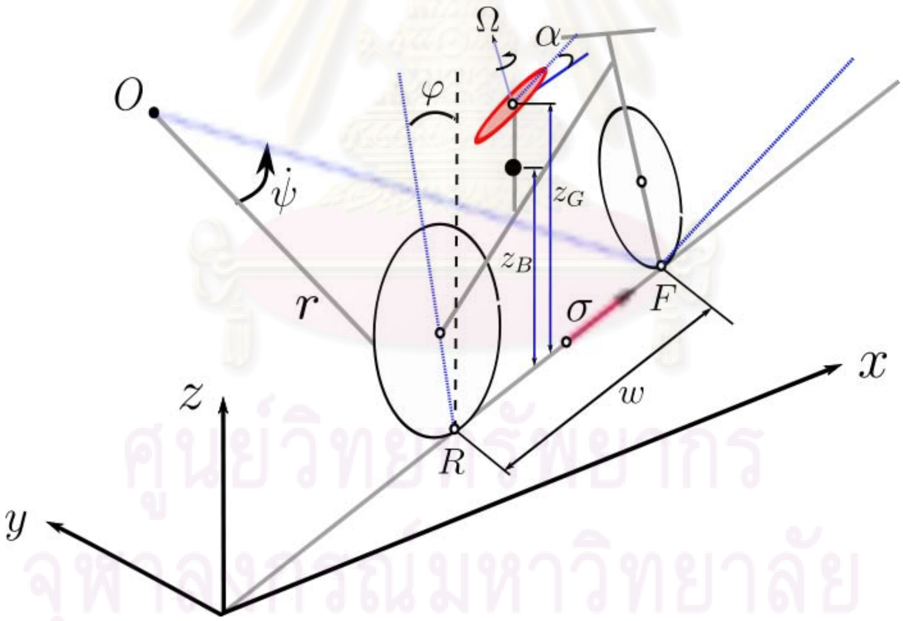

Figure 4.1: The Bicycle Geometry.

Parameter Definition

The parameter notations here are also consistent with the measured parameter in Tables 2.1 and 3.1. We present them separately to emphasize each component; the bicycle dimension, the flywheel (for design calculation), and the bicycle with gyroscopic flywheel model parameters. These are shown in Table 4.1. The constant mass, moment of inertia, and height of the center of mass are obtained via CATIA CAD software. These values in Table 4.1 may differ from Tables 2.1 and 3.1 since we consider the model here in two parts; the body and the flywheel. See more in the bicycle model assumption.

Table 4.1: Parameters for Bicycle Gyroscopic Flywheel Dynamic Model.

Parameter	Symbol	Value	Unit
Bike roll angle	φ	-	rad
Flywheel precession angle	α	-	rad
Bike rotation rate	$\dot{\psi}$	-	rad/s
Flywheel spinning rate	Ω	-	rad/s
Track radius curvature	r	-	m
The midpoint of track segment	s	-	m
The distance between s and wheelbase midpoint	h	-	m
The wheelbase midpoint speed	σ	-	m/s
Disturbance force	F_d	-	N
Bicycle body mass	m_B	30	kg
Flywheel mass	m_G	9	kg
Height of Bicycle center of mass	z_G	0.39	m
Height of Flywheel center of mass	z_B	0.88	m
Bike Moment of inertia	$(I_{Bxx}, I_{Byy}, I_{Bzz})$	(5.947,8.083,2.295)	kg$\cdot$ m^2
Flywheel Moment of inertia	$(I_{Gxx}, I_{Gyy}, I_{Gzz})$	(0.138,0.138,0.274)	kg$\cdot$ m^2

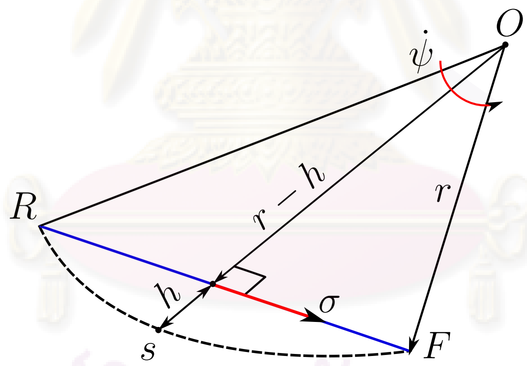

Figure 4.2: The bicycle curvature path.

To explain more about the curvature path of the bicycle, see Figure 4.2. In Figure, F is the front wheel ground contact point, R is the rear wheel ground contact point, and O is the center point of rotation. The distance between R and F is called "wheelbase length " (w). We can find the relation between $\dot{s}$ and $\dot{\psi}$ is $\sigma = \dot{s}(r-h)/r = \dot{\psi}(r-h)$. For straight path running, $r \to \infty$, $h = 0$ and $\sigma = \dot{s}$.

4.2 Model Assumptions

It is much more complex to treat the bicycle model as a 3D rigid body. The simplified model that captured the major effects on the bicycle and is well enough to describe the bicycle dynamics is a better choice. However, we should be careful to define the assumption and its limitation as shown below.

- The steering axis has no trail.
- The bicycle is rolling on a flat plane
- The tires has no width and no deformation.
- The longitudinal and lateral slips at the front and rear wheel are neglected.
- The bicycle is considered as a point mass at the center of mass height z_B
- The flywheel is considered as a point mass at the center of mass height z_G
- The mass moment of inertia of the front and rear wheel are neglected.

4.2.1 Nonlinear Dynamic Model

The model derivation is done by Lagrangian method. We follow the derivation in [2] but we combine the load and flywheel cage into the bicycle body in one point mass. The kinetic energy of the system is

$$T = \frac{1}{2} m_B \mathbf{v}_B^T \mathbf{v}_B + \frac{1}{2} \omega_B^T \mathbf{I_B} \omega_B + \frac{1}{2} m_G \mathbf{v}_G^T \mathbf{v}_G + \frac{1}{2} \omega_G^T \mathbf{I_G} \omega_G \tag{4.1}$$

and the potential energy of the system is

$$V = (m_B z_B + m_G z_G) g \sin\varphi \tag{4.2}$$

where

$$\omega_B = \begin{bmatrix} \dot{\varphi} \\ \dot{\psi}\sin\varphi \\ \dot{\psi}\cos\varphi \end{bmatrix} \qquad \mathbf{v}_B = \begin{bmatrix} \sigma + (\dot{\psi}\sin\varphi) z_B \\ \dot{\varphi} z_B \\ 0 \end{bmatrix}$$

$$\omega_\mathbf{G} = \begin{bmatrix} \dot{\varphi}\cos\alpha - \dot{\psi}\cos\varphi\sin\alpha \\ \dot{\psi}\sin\varphi + \dot{\alpha} \\ \dot{\varphi}\sin\alpha + \dot{\psi}\cos\varphi\cos\alpha + \Omega \end{bmatrix} \qquad \mathbf{v}_G = \begin{bmatrix} \sigma + (\dot{\psi}\sin\varphi) z_G \\ \dot{\varphi} z_G \\ 0 \end{bmatrix}$$

From the Lagrangian $\mathcal{L}(q,\dot{q}) \equiv T(q,\dot{q}) - V(q)$, we can derive the Lagrange's equations in the form

$$\frac{d}{dt}\left(\frac{\partial \mathcal{L}}{\partial \dot{q}_k}\right) - \frac{\partial \mathcal{L}}{\partial q_k} = Q_k \tag{4.3}$$

where the generalized coordinates are

$$\begin{cases} q_1 & : \ \varphi \text{ (Bike roll angle)} \\ q_2 & : \ \alpha \text{ (Flywheel precession angle)} \end{cases}$$

and the generalized forces are

$$\begin{cases} Q_1 & = \ F_d z_B \cos\varphi \\ Q_2 & = \ T_\alpha \end{cases}$$

According to (4.3), the equation of motions are obtained as follow:

Bicycle rolling equation

$$\left.\begin{aligned}&(k_9 + k_4\cos^2\alpha + k_6\sin^2\alpha)\ddot{\varphi}\\ &-2k_{10}\dot{\varphi}\dot{\alpha}\sin\alpha\cos\alpha\\ &+\dot{\psi}\dot{\alpha}\cos\varphi(k_{10}(\sin^2\alpha - \cos^2\alpha) - k_5)\\ &-\dot{\psi}^2\cos\varphi\sin\varphi(k_{11} - k_4\sin^2\alpha - k_6\cos^2\alpha)\\ &+(\Omega I_{Gzz}\cos\alpha)\dot{\alpha}\\ &+\dot{\psi}\Omega I_{Gzz}\cos\alpha\sin\varphi\\ &-k_7 g\sin\varphi\end{aligned}\right\} = k_7\sigma\dot{\psi}\cos\varphi + F_d z_B\cos\varphi \tag{4.4}$$

Flywheel precessing equation

$$\left.\begin{aligned}&k_5\ddot{\alpha}\\ &+k_5\dot{\psi}\dot{\varphi}\cos\varphi\\ &+k_{10}(\dot{\varphi}^2\cos\alpha\sin\alpha - \dot{\psi}^2\cos^2\varphi\cos\alpha\sin\alpha - \dot{\psi}\dot{\varphi}\cos\varphi(\sin^2\alpha - \cos^2\alpha))\\ &+\Omega(\dot{\psi}\cos\varphi\sin\alpha - \dot{\varphi}\cos\alpha)I_{Gzz}\end{aligned}\right\} = T_\alpha \tag{4.5}$$

where

$$\begin{array}{ll} k_1 = I_{Bxx} & k_2 = I_{Byy} \\ k_3 = I_{Bzz} & k_4 = I_{Gxx} \\ k_5 = I_{Gyy} & k_6 = I_{Gzz} \\ k_7 = m_B z_B + m_G z_G & k_8 = m_B z_B^2 + m_G z_G^2 \\ k_9 = k_1 + k_8 & k_{10} = k_4 - k_6 \\ k_{11} = k_8 + k_2 - k_3 + k_5 & \end{array}$$

4.3 Linearized Dynamic Model

The conventional simple way to deal with the nonlinear system is to linearize the nonlinear system around its equilibrium point. We will use this linearized model for a comparison with our reduced nonlinear in the next section. Let the state vector

$$x = [\varphi \quad \alpha \quad \dot{\varphi} \quad \dot{\alpha}]^T$$

Linearize the nonlinear model (4.4) and (4.5) about $\mathbf{x} = 0$, then

$$(k_9 + k_4)\ddot{\varphi} - k_7\sigma\dot{\psi} + \Omega I_{Gzz}\dot{\alpha} + \Omega I_{Gzz}\dot{\psi}\varphi = k_7 g\varphi \tag{4.6}$$

$$k_5\ddot{\alpha} + \Omega(\dot{\psi}\alpha - \dot{\varphi})I_{Gzz} = T_\alpha \tag{4.7}$$

Rewrite the above two equations in a state space form

$$\frac{d}{dt}\begin{bmatrix}\varphi\\ \alpha\\ \dot{\varphi}\\ \dot{\alpha}\end{bmatrix} = \begin{bmatrix}0 & 0 & 1 & 0\\ 0 & 0 & 0 & 1\\ a_{31} & 0 & 0 & a_{34}\\ 0 & a_{42} & a_{43} & 0\end{bmatrix}\begin{bmatrix}\varphi\\ \alpha\\ \dot{\varphi}\\ \dot{\alpha}\end{bmatrix} + \begin{bmatrix}0\\ 0\\ \sigma\dot{\psi}k_7/(k_9 + k_4)\\ T_\alpha/k_5\end{bmatrix} \tag{4.8}$$

where

$$a_{31} = \frac{k_7 g - \dot{\psi}\Omega I_{Gzz}}{k_9 + k_4} \qquad a_{34} = \frac{-\Omega I_{Gzz}}{k_9 + k_4}$$

$$a_{42} = -\frac{1}{k_5}(\dot{\psi}\Omega I_{Gzz}) \qquad a_{43} = \frac{\Omega I_{Gzz}}{k_5}$$

CHAPTER V

PIECEWISE AFFINE MODEL FOR BICYCLE ROBOT

In order to synthesis the controller by PWQ stabilization technique, one needs to model the nonlinear system dynamics to be the PWA model with the error as small as possible. In this chapter, we describe how to obtain the PWA model by a simple trigonometric terms approximation method, least-square-error without boundary constraints, and least-square-error without boundary constraints.

We starts with defining the regions that will be approximated by PWA model. The bicycle roll angle is partitioned into 3 regions, the flywheel precession angle does so. Thus, the operating regions were split into 9 regions or polyhedral cells, see Fig. 5.1. X_5 is considered to be in I_0 or the steady state point region where the state trajectory rest at the point $(0, 0, 0, 0)$ when the system is made stable. The other cells X_i are in the set I_1. Note that these 9 regions is not the best choice to reduce model error. More regions lead to more accurate model but more calculation is needed.

The nonlinear differential equations (4.4) and (4.5) can be approximated by continuous PWA functions into the state-space form (2.7). We define the parameters for our bicycle robot model as

$$x = \begin{bmatrix} \varphi \\ \alpha \\ \dot{\varphi} \\ \dot{\alpha} \end{bmatrix} \qquad u = T_\alpha \qquad A_i = \begin{bmatrix} 0 & 0 & 1 & 0 \\ 0 & 0 & 0 & 1 \\ A_{31}^{(i)} & A_{32}^{(i)} & A_{33}^{(i)} & A_{34}^{(i)} \\ A_{41}^{(i)} & A_{42}^{(i)} & A_{43}^{(i)} & A_{44}^{(i)} \end{bmatrix} \qquad a_i = \begin{bmatrix} 0 \\ 0 \\ a_{3a}^{(i)} \\ a_{4a}^{(i)} \end{bmatrix} \qquad B_i = \begin{bmatrix} 0 \\ 0 \\ 0 \\ B_{41}^{(i)} \end{bmatrix}$$

Next, the PWA model approximation methods will be shown from a simple method (fast calculation but roughly accuracy) to the more complex (longer time for calculation but more accuracy) method. All constant terms are taken from Table 4.1.

5.1 Trigonometric Terms Approximation

We approximate the nonlinear terms sin and cos by least square error method in each interval, while the other nonlinear terms are approximated by linearization about the operationg point $(0, 0, 0, 0)$.

- Approximate the nonlinear terms sin and cos by least square error method and use 'θ' to represent φ and α only for this occasion as follow
  - When $\theta \le -0.1745$, we approximate $\sin\theta \approx m_1(\theta + 0.1745)$ and $\cos\theta \approx m_2(\theta + 0.1745)$,

$$m_1 = \text{argmin} \int_{-1.0472}^{-0.1745} (m_1(\theta + 0.1745) - 0.1745 - \sin\theta)^2 d\theta$$
$$m_2 = \text{argmin} \int_{-1.0472}^{-0.1745} (m_2(\theta + 0.1745) + 1 - \cos\theta)^2 d\theta$$

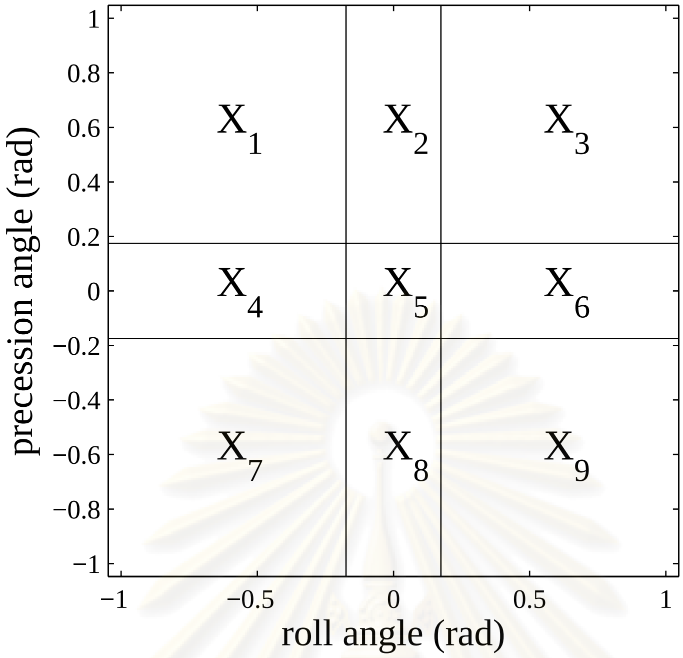

Figure 5.1: Polyhedral partition of the PWA bicycle state space model.

*The calculation is done only in the range $-1.0472 \leq \theta \leq -0.1745$ or $-60^\circ \leq \theta \leq -10^\circ$.

- When $-0.1745 \leq \theta \leq 0.1745$, we linearize $\sin\theta$ and $\cos\theta$ around $\theta = 0$,

$$\sin\theta \approx \theta \qquad\qquad \cos\theta \approx 1$$

- When $\theta \geq 0.1745$, we approximate $\sin\theta \approx m_3(\theta - 0.1745)$ and $\cos\theta \approx m_4(\theta - 0.1745)$,

$$m_3 = \text{argmin} \int_{0.1745}^{1.0472} (m_3(\theta - 0.1745) + 0.1745 - \sin\theta)^2 d\theta$$
$$m_4 = \text{argmin} \int_{0.1745}^{1.0472} (m_4(\theta - 0.1745) + 1 - \cos\theta)^2 d\theta$$

*The calculation is done only in the range $-1.0472 \leq \theta \leq -0.1745$ or $10^\circ \leq \theta \leq 60^\circ$.

Finally,

$$\sin\theta \approx \begin{cases} 0.85558\theta - 0.02516 & \theta \leq -0.1745 \\ \theta & -0.1745 \leq \theta \leq 0.1745 \\ 0.85558\theta + 0.02516 & \theta \geq 0.1745 \end{cases} \tag{5.1}$$

$$\cos\theta \approx \begin{cases} 0.4957\theta + 1.0865 & \theta \leq -0.1745 \\ 1 & -0.1745 \leq \theta \leq 0.1745 \\ -0.4957\theta + 1.0865 & \theta \geq 0.1745 \end{cases} \tag{5.2}$$

- Substitute the approximated functions from (5.1) and (5.2) shown below into (4.4) and (4.5).

$$\sin\alpha \approx a_{1i}\alpha + b_{1i} \qquad \cos\alpha \approx a_{2i}\alpha + b_{2i}$$
$$\sin\varphi \approx a_{3i}\varphi + b_{3i} \qquad \cos\varphi \approx a_{4i}\varphi + b_{4i}$$

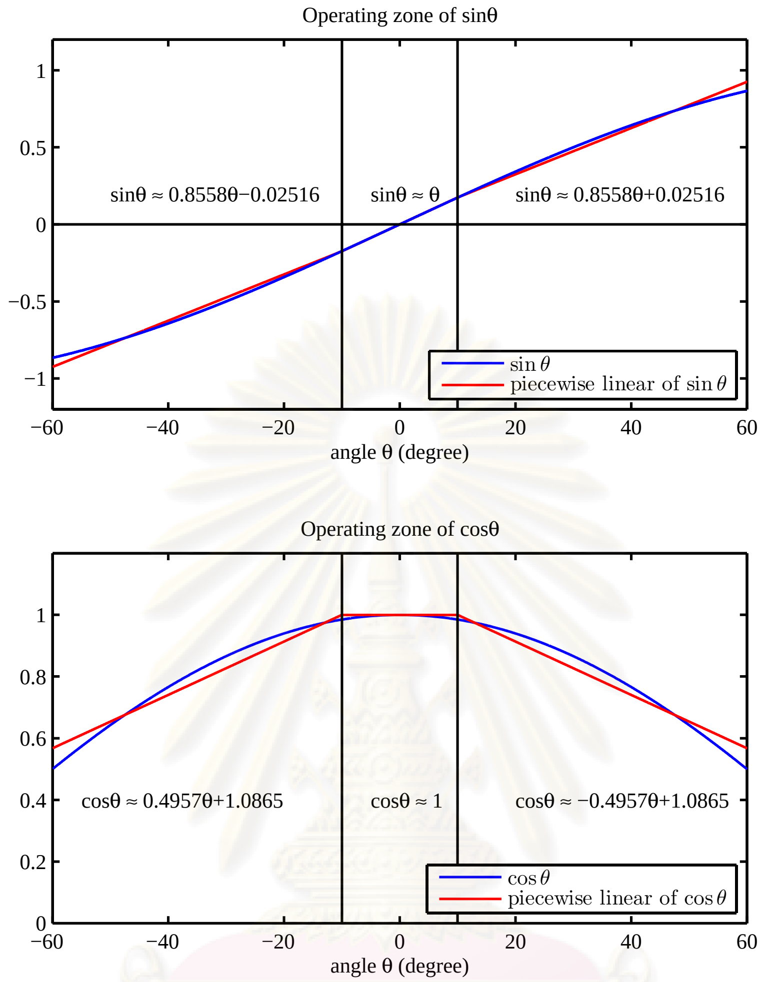

Figure 5.2: Affine approximation of functions sin and cos.

where $i = 1, \ldots, 9$ indicated the region of approximation.

- Approximate the higher order terms and other nonlinear terms of $\dot{\alpha}$ and $\dot{\varphi}$ based on linearization about the operating point $(\alpha, \dot{\alpha}, \varphi, \dot{\varphi}) = (0, 0, 0, 0)$ into the state-space form (2.7) where

$$\begin{aligned}
A_{31}^{(i)} &= (K_9^{(i)} + K_{11}^{(i)} - K_3^{(i)} - K_7^{(i)})/K_1^{(i)} \\
A_{32}^{(i)} &= -(K_4^{(i)} + K_6^{(i)})/K_1^{(i)} \\
A_{33}^{(i)} &= 0 \\
A_{34}^{(i)} &= -(K_2^{(i)} + K_5^{(i)})/K_1^{(i)} \\
a_{3a}^{(i)} &= (K_{10}^{(i)} - K_8^{(i)} - K_{22}^{(i)})/K_1^{(i)}
\end{aligned}$$

$$\begin{aligned}
A_{41}^{(i)} &= -(K_{14}^{(i)} + K_{18}^{(i)})/k_5 \\
A_{42}^{(i)} &= -(K_{21}^{(i)} + K_{15}^{(i)})/k_5 \\
A_{43}^{(i)} &= -(K_{13}^{(i)} + K_{17}^{(i)} + K_{20}^{(i)})/k_5 \\
A_{44}^{(i)} &= 0 \\
a_{4a}^{(i)} &= -(K_{16}^{(i)} + K_{19}^{(i)})/k_5 \\
B_{41}^{(i)} &= 1/k_5
\end{aligned}$$

Table 5.1: Approximated trigonometric functions in each polyhedral cell.

$\alpha \uparrow$	$\varphi < -10^\circ$	$-10^\circ \le \varphi \le 10^\circ$	$\varphi > 10^\circ$ $\rightarrow \varphi$
$\alpha > 10^\circ$	$\sin\alpha \approx 0.8558\alpha + 0.02516$ $\cos\alpha \approx -0.4957\alpha + 1.0865$ $\sin\varphi \approx 0.8558\varphi - 0.02516$ $\cos\varphi \approx 0.4957\varphi + 1.0865$	$\sin\alpha \approx 0.8558\alpha + 0.02516$ $\cos\alpha \approx -0.4957\alpha + 1.0865$ $\sin\varphi \approx \varphi$ $\cos\varphi \approx 1$	$\sin\alpha \approx 0.8558\alpha + 0.02516$ $\cos\alpha \approx -0.4957\alpha + 1.0865$ $\sin\varphi \approx 0.8558\varphi + 0.02516$ $\cos\varphi \approx -0.4957\varphi + 1.0865$
$-10^\circ \le \alpha \le 10^\circ$	$\sin\alpha \approx \alpha$ $\cos\alpha \approx 1$ $\sin\varphi \approx 0.8558\varphi - 0.02516$ $\cos\varphi \approx 0.4957\varphi + 1.0865$	$\sin\alpha \approx \alpha$ $\cos\alpha \approx 1$ $\sin\varphi \approx \varphi$ $\cos\varphi \approx 1$	$\sin\alpha \approx \alpha$ $\cos\alpha \approx 1$ $\sin\varphi \approx 0.8558\varphi + 0.02516$ $\cos\varphi \approx -0.4957\varphi + 1.0865$
$\alpha < -10^\circ$	$\sin\alpha \approx 0.8558\alpha - 0.02516$ $\cos\alpha \approx 0.4957\alpha + 1.0865$ $\sin\varphi \approx 0.8558\varphi - 0.02516$ $\cos\varphi \approx 0.4957\varphi + 1.0865$	$\sin\alpha \approx 0.8558\alpha - 0.02516$ $\cos\alpha \approx 0.4957\alpha + 1.0865$ $\sin\varphi \approx \varphi$ $\cos\varphi \approx 1$	$\sin\alpha \approx 0.8558\alpha - 0.02516$ $\cos\alpha \approx 0.4957\alpha + 1.0865$ $\sin\varphi \approx 0.8558\varphi + 0.02516$ $\cos\varphi \approx -0.4957\varphi + 1.0865$

$$
\begin{aligned}
K_1^{(i)} &= (k_9 + k_4 b_{2i}^2 + k_6 b_{1i}^2) & K_2^{(i)} &= \dot\psi b_{4i}(k_{10}(b_{1i}^2 - b_{2i}^2) - k_5) \\
K_3^{(i)} &= -\dot\psi^2(a_{3i}b_{4i} + a_{4i}b_{3i})(k_{11} - k_4 b_{1i}^2 - k_6 b_{2i}^2) & K_4^{(i)} &= -\dot\psi^2 b_{3i}b_{4i}(-2k_4 a_{1i}b_{1i} - 2k_6 a_{2i}b_{2i}) \\
K_5^{(i)} &= \Omega I_{Gzz} b_{2i} & K_6^{(i)} &= \dot\psi\Omega I_{Gzz}(a_{2i}b_{3i}) \\
K_7^{(i)} &= \dot\psi\Omega I_{Gzz}(a_{3i}b_{2i}) & K_8^{(i)} &= \dot\psi\Omega I_{Gzz}(b_{3i}b_{2i}) \\
K_9^{(i)} &= k_7 g a_{3i} & K_{10}^{(i)} &= k_7 g b_{3i} \\
K_{11}^{(i)} &= k_7\sigma\dot\psi a_{4i} & K_{12}^{(i)} &= k_7\sigma\dot\psi b_{4i} \\
K_{13}^{(i)} &= k_5\dot\psi b_{4i} & K_{14}^{(i)} &= -k_{10}\dot\psi^2(2a_{4i}b_{4i}b_{1i}b_{2i}) \\
K_{15}^{(i)} &= -k_{10}\dot\psi^2(a_{1i}b_{2i} + a_{2i}b_{1i})b_{4i}^2 & K_{16}^{(i)} &= -k_{10}\dot\psi^2 b_{1i}b_{2i}b_{4i}^2 \\
K_{17}^{(i)} &= -k_{10}\dot\psi b_4(b_{1i}^2 - b_{2i}^2) & K_{18}^{(i)} &= \Omega\dot\psi I_{Gzz}(a_{4i}b_{1i}) \\
K_{19}^{(i)} &= \Omega\dot\psi I_{Gzz}(b_{1i}b_{4i}) & K_{20}^{(i)} &= -\Omega I_{Gzz} b_{2i} \\
K_{21}^{(i)} &= \Omega\dot\psi I_{Gzz}(a_{1i}b_{4i}) & K_{22}^{(i)} &= -\dot\psi^2 b_{3i}b_{4i}(k_{11} - k_4 b_{1i}^2 - k_6 b_{2i}^2)
\end{aligned}
$$

- Substitute the bicycle parameters in the Table 4.1 and get the resulting system matrices

5.2 Least-Square Error Approximation without Boundary Constraints

This approximation method gives a discontinuous model at the cell boundaries since the error is forced to be minimized while nothing concerning with the boundary constraints are taken into account. To approximate the nonlinear terms of $\ddot\alpha$ and $\ddot\varphi$ into a state-space form, we formulate the least square problem from the proposed approximated linear model :

$$\ddot{y}_{N\times 1} = G_{N\times m}\theta_{m\times 1} + \mu_{N\times 1} \tag{5.3}$$

where

$$\begin{aligned}
G &= \begin{bmatrix} x_1 & x_2 & x_3 & x_4 & 1 \end{bmatrix} \\
\theta_\varphi &= \begin{bmatrix} A^{(i)}_{31} & A^{(i)}_{32} & A^{(i)}_{33} & A^{(i)}_{34} & a^{(i)}_{3} \end{bmatrix}^T \text{ or} \\
\theta_\alpha &= \begin{bmatrix} A^{(i)}_{41} & A^{(i)}_{42} & A^{(i)}_{43} & A^{(i)}_{44} & a^{(i)}_{4} \end{bmatrix}^T
\end{aligned}$$

$\ddot{y}$ is the exact value of $\ddot{\varphi}$ or $\ddot{\alpha}$ obtained from the bicycle dynamic equation (4.4) and (4.5)
μ is the approximation error
x_k is the k^{th} vector containing N realizations of a uniform random variable in the range $[x_{k_{min}}, x_{k_{max}}]$ in each X_i
N is the number of realization (higher is better)
m is the number the state plus a single affine term

Then we can present the problem as

$$\hat{\theta}^{(i)} = \underset{\theta^{(i)}}{\text{argmin}} \parallel \ddot{y} - G^{(i)}\theta^{(i)} \parallel_2^2 \tag{5.4}$$

Solving (5.4) for each cell, we will get all 9 sets of system matrices of the bicycle PWA model.

5.3 Least-Square Error Approximation with Boundary Constraints

This model is continuous across the boundary. We carefully begin an approximation with the cell $X_5 \in I_0$ in order to made this cell the most accurate. The benefit is that there is no constraint for model continuity at the first approximation in X_5. When the first cell has already been placed, it introduces one more boundary constraint at its attached polyhedral cell. This is in case II and in the same manner for more constraints in case III.

- *Case I: No constraint*

  Formulate the least square problem (5.4) with the same methodology for the operating-point region X_5. The closed form solution is

$$\hat{\theta}^{(5)} = (G^{(5)T}G^{(5)})^{-1}G^{(5)T}\ddot{y} \tag{5.5}$$

- *Case II: One constraint*

  One constraint of the problem is appeared when the approximation is done in the nearby region of X_5 i.e. X_2, X_4, X_6, X_8. Consider an example of X_6, the continuity the model at boundary $x_1 = \gamma$ connecting X_5 to X_6. The solution for $\hat{\theta}^{(6)}$ can be obtained by solving the following problem

$$\begin{aligned}
\text{minimize} \quad & \parallel \ddot{y} - G^{(6)}\theta^{(6)} \parallel_2^2 \\
\text{subject to} \quad & G_\gamma\theta^{(6)} = G_\gamma\theta^{(5)}
\end{aligned} \tag{5.6}$$

  where $G_\gamma = \begin{bmatrix} \gamma & x_2 & x_3 & x_4 & 1 \end{bmatrix}$

  For the rest of X_5 connected regions X_2, X_4, X_6, X_8, the approximation is applied in the similar fashion.

- *Case III: Two constraints*
  Two constraints are taken into account when an approximation is done in the region X_1, X_3, X_7, X_9. Consider the continuity of the model in X_3 at the boundary $x_1 = \gamma$ that connects the region X_2 and X_3 and the boundary $x_2 = \beta$ that connects to the region X_6 and X_3, the problem can be written in this form

$$\begin{array}{ll} \text{minimize} & \| \ddot{y} - G^{(3)}\theta^{(3)} \|_2^2 \\ \text{subject to} & G_\gamma \theta^{(3)} = G_\gamma \theta^{(2)} \\ & G_\beta \theta^{(3)} = G_\beta \theta^{(6)} \end{array} \tag{5.7}$$

$$\text{where} \quad \begin{array}{l} G_\gamma = \begin{bmatrix} \gamma & x_2 & x_3 & x_4 & 1 \end{bmatrix} \\ G_\beta = \begin{bmatrix} x_1 & \beta & x_3 & x_4 & 1 \end{bmatrix} \end{array}$$

In 5.2 and 5.3, the range $[x1_{min}, x1_{max}]$ and $[x2_{min}, x2_{max}]$ are defined upon the region X_i. For the angular velocities as represented by x_3 and x_4, there is no partition region given. Hence, we assign an operating point $(0, 0)$ for them. The approximation of x_1 and x_2 will be varied in each region but x_3 and x_4 will be fixed at $(0, 0)$ which its resulting models are like the linearisation model around this point.

The example of system matrices in each region after substituting constant parameters are shown in the next pages. They are calculated by the assumption that the bicycle rotating velocity and forward velocity are very small and no disturbance force ($F_d = 0$) in the system. Also, the constant terms $\dot{\psi} = 0.01$ rad/s, $\sigma = 0$ m/s, $\Omega = 3000$ rpm $= 314.16$ rad/s, and other values from Table 4.1 are also included.

Trigonometric terms approximation model

$$A_1 = \begin{bmatrix} 0 & 0 & 1 & 0 \\ 0 & 0 & 0 & 1 \\ 9.291 & -0.0006 & 0 & -5.3011 \\ -0.0778 & -5.8 & 677.723 & 0 \end{bmatrix} \quad a_1 = \begin{bmatrix} 0 \\ 0 \\ -0.2732 \\ -0.1705 \end{bmatrix} \quad B_1 = \begin{bmatrix} 0 \\ 0 \\ 0 \\ 7.2464 \end{bmatrix}$$

$$A_2 = \begin{bmatrix} 0 & 0 & 1 & 0 \\ 0 & 0 & 0 & 1 \\ 10.8566 & 0 & 0 & -5.3011 \\ 0 & -5.3383 & 677.7228 & 0 \end{bmatrix} \quad a_2 = \begin{bmatrix} 0 \\ 0 \\ 0 \\ -0.1569 \end{bmatrix} \quad B_2 = \begin{bmatrix} 0 \\ 0 \\ 0 \\ 7.2464 \end{bmatrix}$$

$$A_3 = \begin{bmatrix} 0 & 0 & 1 & 0 \\ 0 & 0 & 0 & 1 \\ 9.291 & 0.0006 & 0 & -5.3011 \\ 0.0778 & -5.8 & 677.723 & 0 \end{bmatrix} \quad a_3 = \begin{bmatrix} 0 \\ 0 \\ 0.2732 \\ -0.1705 \end{bmatrix} \quad B_3 = \begin{bmatrix} 0 \\ 0 \\ 0 \\ 7.2464 \end{bmatrix}$$

$$A_4 = \begin{bmatrix} 0 & 0 & 1 & 0 \\ 0 & 0 & 0 & 1 \\ 9.3079 & 0 & 0 & -4.886 \\ 0 & -6.7773 & 623.7653 & 0 \end{bmatrix} \quad a_4 = \begin{bmatrix} 0 \\ 0 \\ -0.2736 \\ 0 \end{bmatrix} \quad B_4 = \begin{bmatrix} 0 \\ 0 \\ 0 \\ 7.2464 \end{bmatrix}$$

$$A_5 = \begin{bmatrix} 0 & 0 & 1 & 0 \\ 0 & 0 & 0 & 1 \\ 10.8762 & 0 & 0 & -4.886 \\ 0 & -6.2378 & 623.7654 & 0 \end{bmatrix} \quad a_5 = \begin{bmatrix} 0 \\ 0 \\ 0 \\ 0 \end{bmatrix} \quad B_5 = \begin{bmatrix} 0 \\ 0 \\ 0 \\ 7.2464 \end{bmatrix}$$

$$A_6 = \begin{bmatrix} 0 & 0 & 1 & 0 \\ 0 & 0 & 0 & 1 \\ 9.3079 & 0 & 0 & -4.886 \\ 0 & -6.7773 & 623.7653 & 0 \end{bmatrix} \quad a_6 = \begin{bmatrix} 0 \\ 0 \\ 0.2736 \\ 0 \end{bmatrix} \quad B_6 = \begin{bmatrix} 0 \\ 0 \\ 0 \\ 7.2464 \end{bmatrix}$$

$$A_7 = \begin{bmatrix} 0 & 0 & 1 & 0 \\ 0 & 0 & 0 & 1 \\ 9.291 & 0.0006 & 0 & -5.3011 \\ 0.0778 & -5.8 & 677.723 & 0 \end{bmatrix} \quad a_7 = \begin{bmatrix} 0 \\ 0 \\ -0.2732 \\ 0.1705 \end{bmatrix} \quad B_7 = \begin{bmatrix} 0 \\ 0 \\ 0 \\ 7.2464 \end{bmatrix}$$

$$A_8 = \begin{bmatrix} 0 & 0 & 1 & 0 \\ 0 & 0 & 0 & 1 \\ 10.8566 & 0 & 0 & -5.3011 \\ 0 & -5.3383 & 677.7228 & 0 \end{bmatrix} \quad a_8 = \begin{bmatrix} 0 \\ 0 \\ 0 \\ 0.1569 \end{bmatrix} \quad B_8 = \begin{bmatrix} 0 \\ 0 \\ 0 \\ 7.2464 \end{bmatrix}$$

$$A_9 = \begin{bmatrix} 0 & 0 & 1 & 0 \\ 0 & 0 & 0 & 1 \\ 9.291 & -0.0006 & 0 & -5.3011 \\ -0.0778 & -5.8 & 677.723 & 0 \end{bmatrix} \quad a_9 = \begin{bmatrix} 0 \\ 0 \\ 0.2732 \\ 0.1705 \end{bmatrix} \quad B_9 = \begin{bmatrix} 0 \\ 0 \\ 0 \\ 7.2464 \end{bmatrix}$$

$C_i = 0 \qquad c_i = 0 \qquad D_i = 0$

$I_0 = \{5\} \qquad I_1 = \{1, 2, 3, 4, 6, 7, 8, 9\}$

Least-square error approximation without boundary constraints model – Discontinuous model

$$A_1 = \begin{bmatrix} 0 & 0 & 1 & 0 \\ 0 & 0 & 0 & 1 \\ 8.7185 & 0.0357 & -0.0015 & -3.862 \\ -1.6106 & -3.7379 & 494.975 & 0.1775 \end{bmatrix} \quad a_1 = \begin{bmatrix} 0 \\ 0 \\ -0.7247 \\ -1.6888 \end{bmatrix} \quad B_1 = \begin{bmatrix} 0 \\ 0 \\ 0 \\ 7.2464 \end{bmatrix}$$

$$A_2 = \begin{bmatrix} 0 & 0 & 1 & 0 \\ 0 & 0 & 0 & 1 \\ 10.8284 & 0.0011 & 0.0053 & -3.87 \\ 0.717 & -5.586 & 495.2182 & -0.671 \end{bmatrix} \quad a_2 = \begin{bmatrix} 0 \\ 0 \\ 0.0026 \\ 0.0386 \end{bmatrix} \quad B_2 = \begin{bmatrix} 0 \\ 0 \\ 0 \\ 7.2464 \end{bmatrix}$$

$$A_3 = \begin{bmatrix} 0 & 0 & 1 & 0 \\ 0 & 0 & 0 & 1 \\ 8.7356 & -0.019 & -0.0014 & -3.8658 \\ 0.5886 & -3.0051 & 495.1564 & 0.1435 \end{bmatrix} \quad a_3 = \begin{bmatrix} 0 \\ 0 \\ 0.7089 \\ -1.2207 \end{bmatrix} \quad B_3 = \begin{bmatrix} 0 \\ 0 \\ 0 \\ 7.2464 \end{bmatrix}$$

$$A_4 = \begin{bmatrix} 0 & 0 & 1 & 0 \\ 0 & 0 & 0 & 1 \\ 8.7439 & -0.0007 & -0.0001 & -4.8606 \\ -0.0724 & -4.9344 & 620.5933 & -0.0131 \end{bmatrix} \quad a_4 = \begin{bmatrix} 0 \\ 0 \\ -0.7004 \\ -0.055 \end{bmatrix} \quad B_4 = \begin{bmatrix} 0 \\ 0 \\ 0 \\ 7.2464 \end{bmatrix}$$

$$A_5 = \begin{bmatrix} 0 & 0 & 1 & 0 \\ 0 & 0 & 0 & 1 \\ 10.8427 & 0.0001 & 0.0001 & -4.861 \\ -0.0354 & -6.0111 & 620.6116 & -0.0106 \end{bmatrix} \quad a_5 = \begin{bmatrix} 0 \\ 0 \\ 0 \\ 0 \end{bmatrix} \quad B_5 = \begin{bmatrix} 0 \\ 0 \\ 0 \\ 7.2464 \end{bmatrix}$$

$$A_6 = \begin{bmatrix} 0 & 0 & 1 & 0 \\ 0 & 0 & 0 & 1 \\ 8.7377 & -0.0044 & -0.0004 & -4.8619 \\ -0.0269 & -4.9932 & 620.6132 & 0.0017 \end{bmatrix} \quad a_6 = \begin{bmatrix} 0 \\ 0 \\ 0.7045 \\ 0.0196 \end{bmatrix} \quad B_6 = \begin{bmatrix} 0 \\ 0 \\ 0 \\ 7.2464 \end{bmatrix}$$

$$A_7 = \begin{bmatrix} 0 & 0 & 1 & 0 \\ 0 & 0 & 0 & 1 \\ 8.7356 & -0.0484 & 0.002 & -3.8671 \\ 1.4033 & -5.4668 & 494.6352 & -0.2225 \end{bmatrix} \quad a_7 = \begin{bmatrix} 0 \\ 0 \\ -0.7257 \\ 0.435 \end{bmatrix} \quad B_7 = \begin{bmatrix} 0 \\ 0 \\ 0 \\ 7.2464 \end{bmatrix}$$

$$A_8 = \begin{bmatrix} 0 & 0 & 1 & 0 \\ 0 & 0 & 0 & 1 \\ 10.7681 & 0.014 & 0.0001 & -3.8668 \\ 6.6803 & -3.2871 & 494.709 & -0.0058 \end{bmatrix} \quad a_8 = \begin{bmatrix} 0 \\ 0 \\ 0.0061 \\ 0.7354 \end{bmatrix} \quad B_8 = \begin{bmatrix} 0 \\ 0 \\ 0 \\ 7.2464 \end{bmatrix}$$

$$A_9 = \begin{bmatrix} 0 & 0 & 1 & 0 \\ 0 & 0 & 0 & 1 \\ 8.7063 & 0.014 & -0.0018 & -3.8661 \\ -2.721 & -6.1022 & 494.6512 & 0.0637 \end{bmatrix} \quad a_9 = \begin{bmatrix} 0 \\ 0 \\ 0.7192 \\ 0.8622 \end{bmatrix} \quad B_9 = \begin{bmatrix} 0 \\ 0 \\ 0 \\ 7.2464 \end{bmatrix}$$

$$C_i = 0 \qquad c_i = 0 \qquad D_i = 0$$

$$I_0 = \{5\} \qquad I_1 = \{1, 2, 3, 4, 6, 7, 8, 9\}$$

Least-square error approximation with boundary constraints model – Continuous model

$$A_1 = \begin{bmatrix} 0 & 0 & 1 & 0 \\ 0 & 0 & 0 & 1 \\ 9.3186 & 0.0104 & 0.0001 & -4.861 \\ 0.011 & -6.2415 & 620.6116 & -0.0106 \end{bmatrix} \quad a_1 = \begin{bmatrix} 0 \\ 0 \\ -0.2678 \\ 0.0483 \end{bmatrix} \quad B_1 = \begin{bmatrix} 0 \\ 0 \\ 0 \\ 7.2464 \end{bmatrix}$$

$$A_2 = \begin{bmatrix} 0 & 0 & 1 & 0 \\ 0 & 0 & 0 & 1 \\ 10.8427 & 0.0104 & 0.0001 & -4.861 \\ -0.0354 & -6.2415 & 620.6116 & -0.0106 \end{bmatrix} \quad a_2 = \begin{bmatrix} 0 \\ 0 \\ -0.0018 \\ 0.0402 \end{bmatrix} \quad B_2 = \begin{bmatrix} 0 \\ 0 \\ 0 \\ 7.2464 \end{bmatrix}$$

$$A_3 = \begin{bmatrix} 0 & 0 & 1 & 0 \\ 0 & 0 & 0 & 1 \\ 9.3166 & 0.0104 & 0.0001 & -4.861 \\ 0.0088 & -6.2415 & 620.6116 & -0.0106 \end{bmatrix} \quad a_3 = \begin{bmatrix} 0 \\ 0 \\ 0.2646 \\ 0.0325 \end{bmatrix} \quad B_3 = \begin{bmatrix} 0 \\ 0 \\ 0 \\ 7.2464 \end{bmatrix}$$

$$A_4 = \begin{bmatrix} 0 & 0 & 1 & 0 \\ 0 & 0 & 0 & 1 \\ 9.3186 & 0.0001 & 0.0001 & -4.861 \\ 0.011 & -6.0111 & 620.6116 & -0.0106 \end{bmatrix} \quad a_4 = \begin{bmatrix} 0 \\ 0 \\ -0.266 \\ 0.0081 \end{bmatrix} \quad B_4 = \begin{bmatrix} 0 \\ 0 \\ 0 \\ 7.2464 \end{bmatrix}$$

$$A_5 = \begin{bmatrix} 0 & 0 & 1 & 0 \\ 0 & 0 & 0 & 1 \\ 10.8427 & 0.0001 & 0.0001 & -4.861 \\ -0.0354 & -6.0111 & 620.6116 & -0.0106 \end{bmatrix} \quad a_5 = \begin{bmatrix} 0 \\ 0 \\ 0 \\ 0 \end{bmatrix} \quad B_5 = \begin{bmatrix} 0 \\ 0 \\ 0 \\ 7.2464 \end{bmatrix}$$

$$A_6 = \begin{bmatrix} 0 & 0 & 1 & 0 \\ 0 & 0 & 0 & 1 \\ 9.3166 & 0.0001 & 0.0001 & -4.861 \\ 0.0088 & -6.0111 & 620.6116 & -0.0106 \end{bmatrix} \quad a_6 = \begin{bmatrix} 0 \\ 0 \\ 0.2664 \\ -0.0077 \end{bmatrix} \quad B_6 = \begin{bmatrix} 0 \\ 0 \\ 0 \\ 7.2464 \end{bmatrix}$$

$$A_7 = \begin{bmatrix} 0 & 0 & 1 & 0 \\ 0 & 0 & 0 & 1 \\ 9.3186 & 0.013 & 0.0001 & -4.861 \\ 0.011 & -2.9629 & 620.6116 & -0.0106 \end{bmatrix} \quad a_7 = \begin{bmatrix} 0 \\ 0 \\ -0.2638 \\ 0.5401 \end{bmatrix} \quad B_7 = \begin{bmatrix} 0 \\ 0 \\ 0 \\ 7.2464 \end{bmatrix}$$

$$A_8 = \begin{bmatrix} 0 & 0 & 1 & 0 \\ 0 & 0 & 0 & 1 \\ 10.8427 & 0.013 & 0.0001 & -4.861 \\ -0.0354 & -2.9629 & 620.6116 & -0.0106 \end{bmatrix} \quad a_8 = \begin{bmatrix} 0 \\ 0 \\ 0.0022 \\ 0.532 \end{bmatrix} \quad B_8 = \begin{bmatrix} 0 \\ 0 \\ 0 \\ 7.2464 \end{bmatrix}$$

$$A_9 = \begin{bmatrix} 0 & 0 & 1 & 0 \\ 0 & 0 & 0 & 1 \\ 9.3166 & 0.013 & 0.0001 & -4.861 \\ 0.0088 & -2.9629 & 620.6116 & -0.0106 \end{bmatrix} \quad a_9 = \begin{bmatrix} 0 \\ 0 \\ 0.2686 \\ 0.5243 \end{bmatrix} \quad B_9 = \begin{bmatrix} 0 \\ 0 \\ 0 \\ 7.2464 \end{bmatrix}$$

$C_i = 0 \qquad c_i = 0 \qquad D_i = 0$

$I_0 = \{5\} \qquad I_1 = \{1, 2, 3, 4, 6, 7, 8, 9\}$

5.4 Comparison of Model Error

The rms errors are calculated from the 10,000 uniform random points within the respected region. The values are collected in the Table 5.4 and Table 5.4. The error in each partitioned region is shown in three dimensions plot in Figures 5.3, 5.4, 5.5, 5.6, 5.7, 5.8, 5.9, and 5.10. The model which has the highest to the lowest error are linearized model, trigonometric terms approximation model, continuous model, and discontinuous model, respectively. This happens to both the bicycle roll angle and flywheel precessing angle. The approximation yields a good result for partitioning the roll angle at $\pm 10^\circ$. Partitioning for more regions will possibly reduce the error.

Table 5.2: Summary of the root-mean-square error of the approximated PWA model.

Bicycle angle

Model region	Linearized	Continuous	Discontinuous	trig. terms approx.
X_1	0.8168	0.2100	0.1537	0.2116
X_2	0.0026	0.0027	0.0036	0.0054
X_3	0.8147	0.2100	0.1528	0.2077
X_4	0.8037	0.2101	0.1533	0.2123
X_5	0.0015	0.0025	0.0013	0.0013
X_6	0.8036	0.2101	0.1534	0.2124
X_7	0.8175	0.2100	0.1532	0.2071
X_8	0.0026	0.0027	0.0070	0.0067
X_9	0.8169	0.2100	0.1539	0.2123
Average	0.5422	0.1409	0.1036	0.1419

Flywheel angle

Model region	Linearized	Continuous	Discontinuous	trig. terms approx.
X_1	1.4861	1.0376	0.3231	1.1844
X_2	0.6506	0.1398	0.2099	0.4688
X_3	1.4574	1.0376	0.4514	1.1873
X_4	0.1816	0.1880	0.0823	0.1117
X_5	0.0310	0.0053	0.0183	0.0183
X_6	0.1817	0.1880	0.0794	0.1118
X_7	1.4642	1.0376	0.4358	0.6338
X_8	0.6498	0.1398	0.9693	1.2216
X_9	1.4905	1.0376	0.6298	0.6384
Average	0.8437	0.5346	0.3555	0.6196

Table 5.3: Summary of the maximum absolute error of the approximated PWA model.

Bicycle angle

Model region	Linearized	Continuous	Discontinuous	trig. terms approx.
X_1	1.9624	0.6175	0.4319	0.6295
X_2	0.0114	0.0128	0.0117	0.0195
X_3	1.9663	0.6175	0.4512	0.6459
X_4	1.9333	0.6033	0.4396	0.6069
X_5	0.0038	0.0099	0.0041	0.0041
X_6	1.9332	0.6033	0.4379	0.6052
X_7	1.9651	0.6175	0.4476	0.6499
X_8	0.0115	0.0128	0.0138	0.0218
X_9	1.9612	0.6175	0.4359	0.6255
Maximum	1.9663	0.6175	0.4512	0.6499

Flywheel angle

Model region	Linearized	Continuous	Discontinuous	trig. terms approx.
X_1	4.1177	3.4618	1.2155	3.7983
X_2	1.4790	0.4272	0.6162	1.1821
X_3	4.0637	3.4618	1.0550	3.7934
X_4	0.6119	0.6413	0.3404	0.5110
X_5	0.0702	0.0220	0.0346	0.0346
X_6	0.6148	0.6413	0.3385	0.5091
X_7	4.0478	3.4618	1.9893	1.6790
X_8	1.4816	0.4272	2.3126	1.7674
X_9	4.1000	3.4618	1.7019	1.6914
Maximum	4.1177	3.4618	2.3126	3.7983

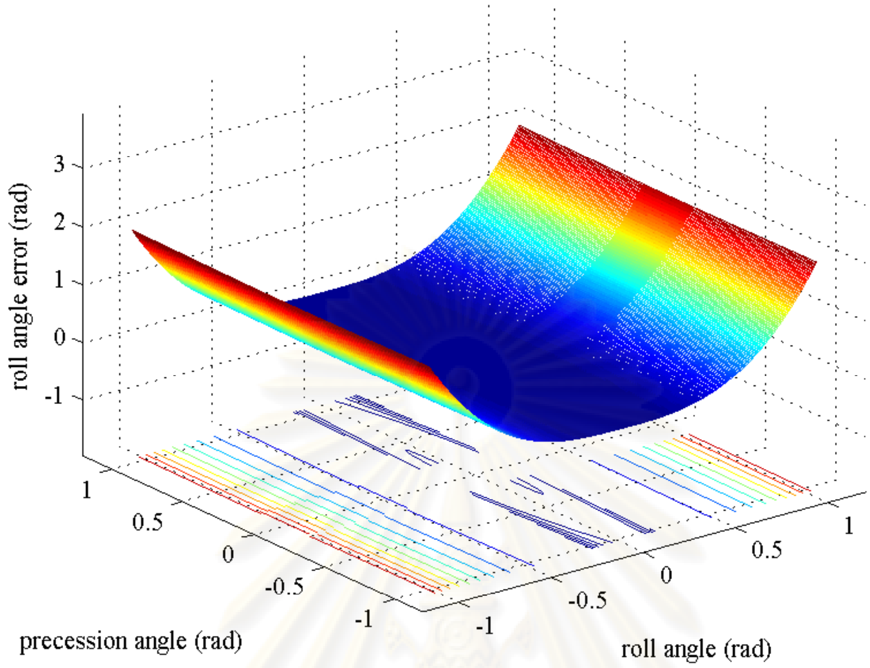

Figure 5.3: The roll angle error plane of the linearized model.

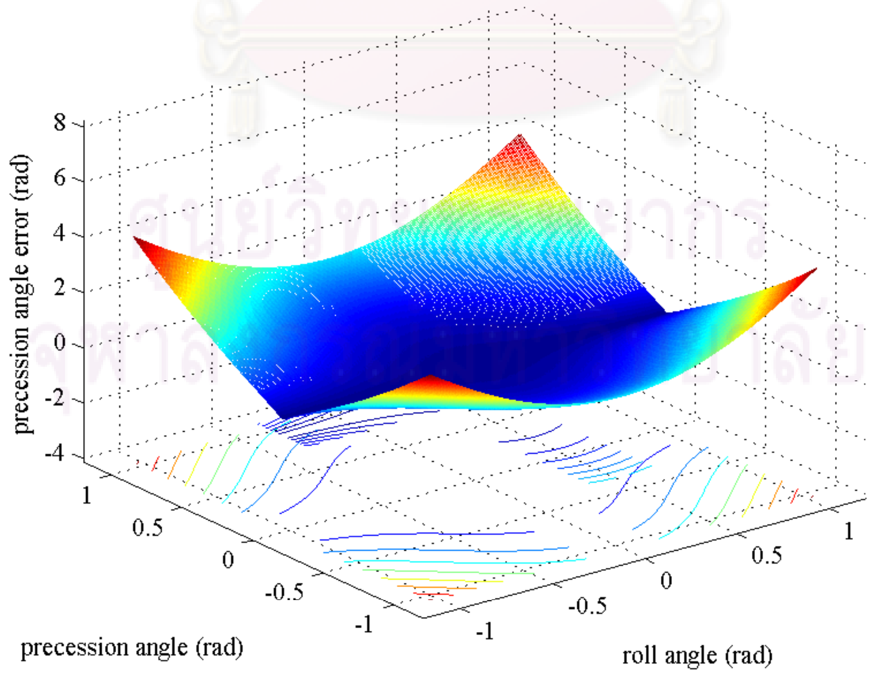

Figure 5.4: The precession angle error plane of the linearized model.

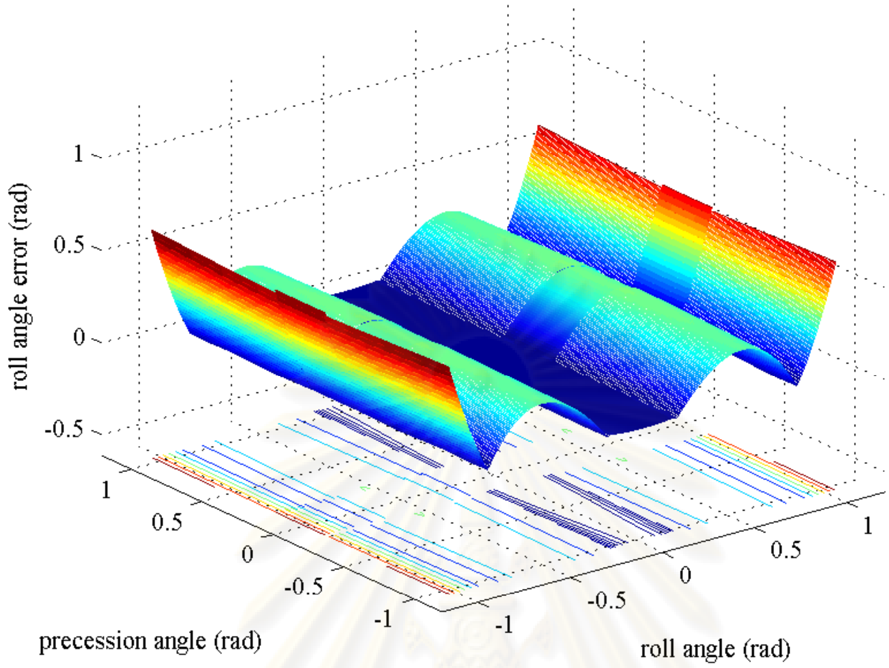

Figure 5.5: The roll angle error plane of the trigonometic terms approximation PWA model.

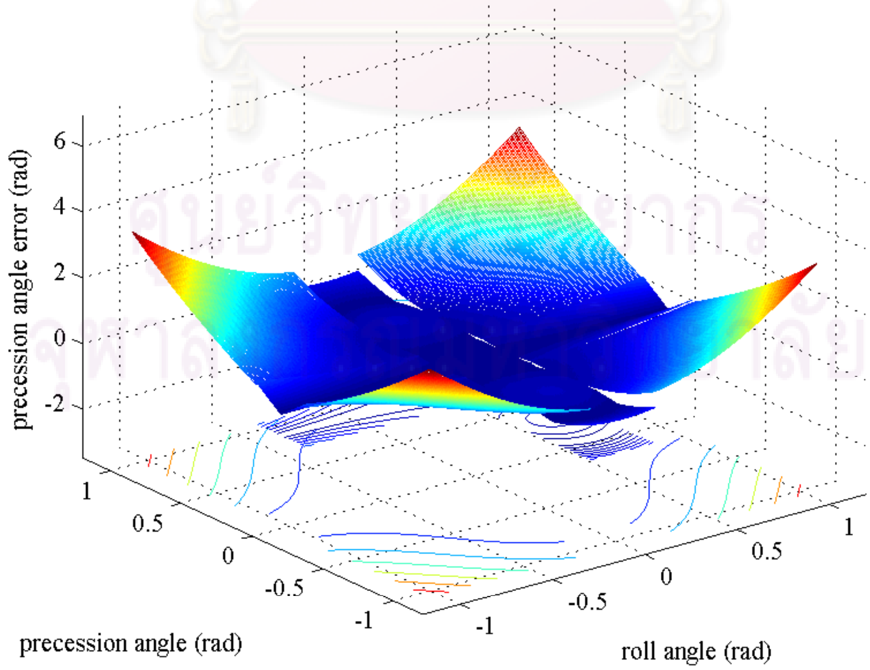

Figure 5.6: The precession angle error plane of the trigonometic terms approximation PWA model.

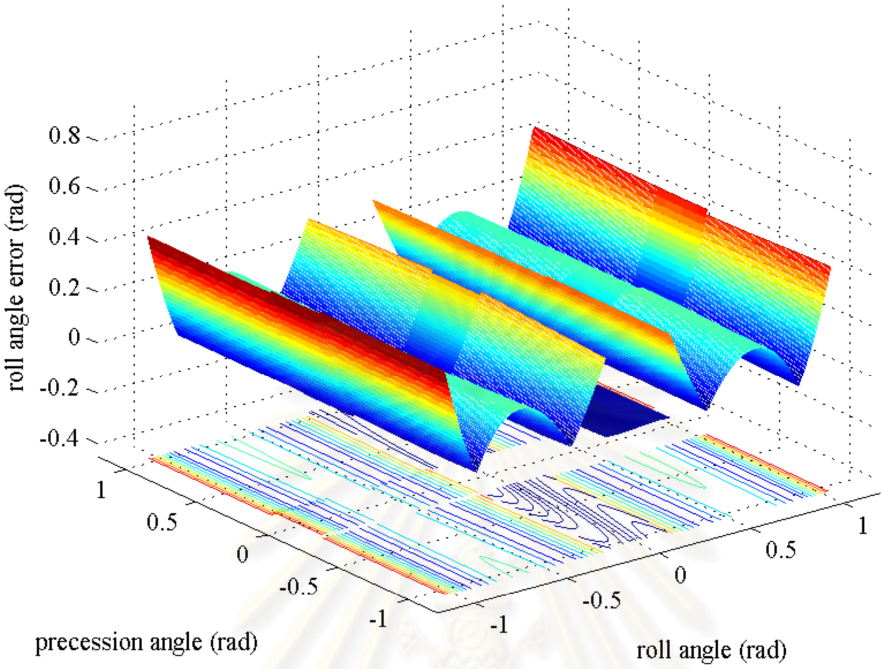

Figure 5.7: The roll angle error plane of the discontinuous PWA model.

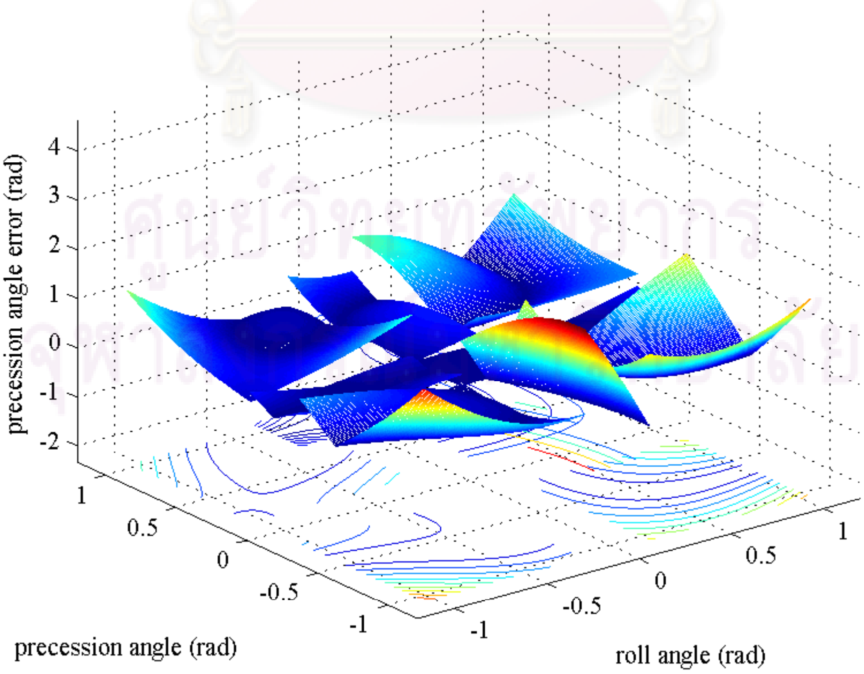

Figure 5.8: The precession angle error plane of the discontinuous PWA model.

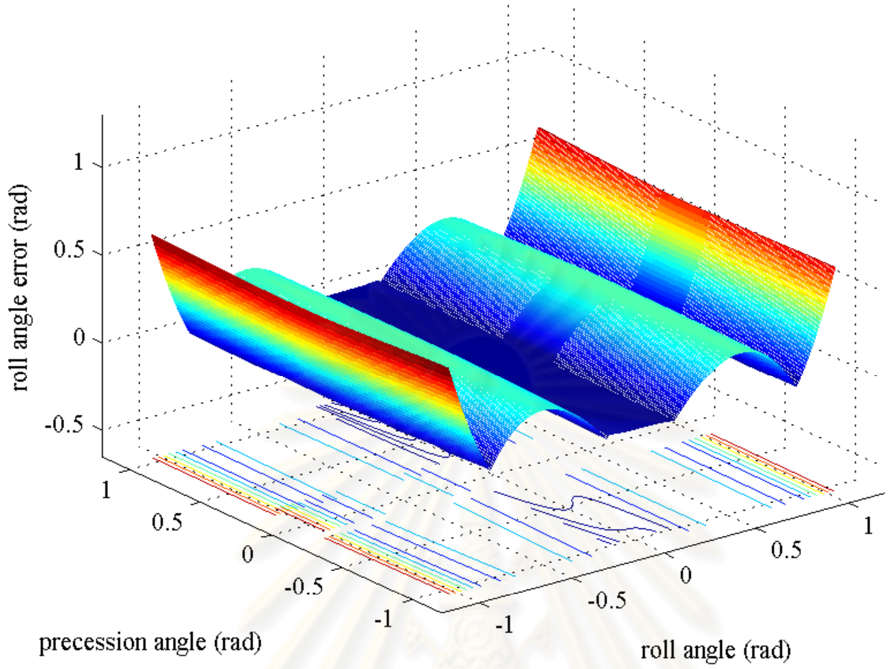

Figure 5.9: The roll angle error plane of the continuous PWA model.

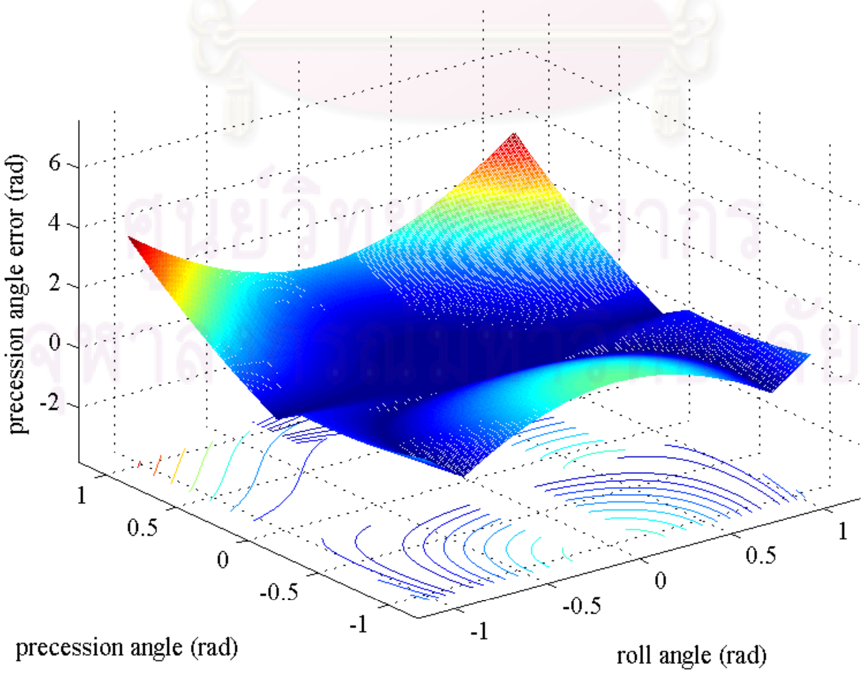

Figure 5.10: The precession angle error plane of the continuous PWA model.

CHAPTER VI

PIECEWISE AFFINE CONTROL FOR BICYCLE ROBOT

The unstable nonlinear bicycle robot system has been already transformed to the PWA system defined by the state-space matrices and cell boundings. This made the stability analysis for the actual nonlinear system easier by searching for the PWQ Lyapunov candidate function of an approximated PWA model. The problem can be cast as a convex optimization problem which has a powerful tool for solving this kind of problem.

In this chapter, we gather all information so far from the beginning to derive the globally quadratic Lypunov function and thus to generate the feedback control laws for system stabilization.

6.1 Problem Formulation

The problem is formulated according to Theorem 2.2. In this problem, we use the discontinuous model which provides the smallest average error value. The system matrices will be brought from Chapter 4. The quadratic cell boundings are computed via the minimum volume outer ellipsoid covering polytopes (see Figure 6.1) problem see the detail in Appendix B. This is the feasibility SDP problem which will be solved using YALMIP [52], the modeling language for advanced modeling and solution of convex and nonconvex optimization problems, which is implemented in MATLAB. The selected solver is SDPT3 [53].

6.2 Main Result

The outcome parameters of solving the problem (2.26) are shown below:

$$
\begin{aligned}
Y \quad &= \begin{bmatrix} -62.444 & -116.74 & 569.69 & 6956.2 \end{bmatrix} \\
Q = \quad Q^T \quad &= \begin{bmatrix} 0.33589 & 0.057914 & -0.98225 & 1.2957 \\ * & 0.56223 & -1.9066 & -3.7011 \\ * & * & 9.2882 & 12.037 \\ * & * & * & 315.32 \end{bmatrix} > 0 \\
L = \quad YQ^{-1} \quad &= \begin{bmatrix} -337.98 & -116.31 & -28.303 & 23.165 \end{bmatrix}
\end{aligned}
$$

The globally quadratic Lyapunov function is $V(x) = x^T P x$ where

$$
P = Q^{-1} = \begin{bmatrix} 9.7037 & 7.7934 & 2.6923 & -0.051174 \\ * & 12.29 & 3.3681 & -0.016343 \\ * & * & 1.1013 & -0.013572 \\ * & * & * & 0.003708 \end{bmatrix} > 0
$$

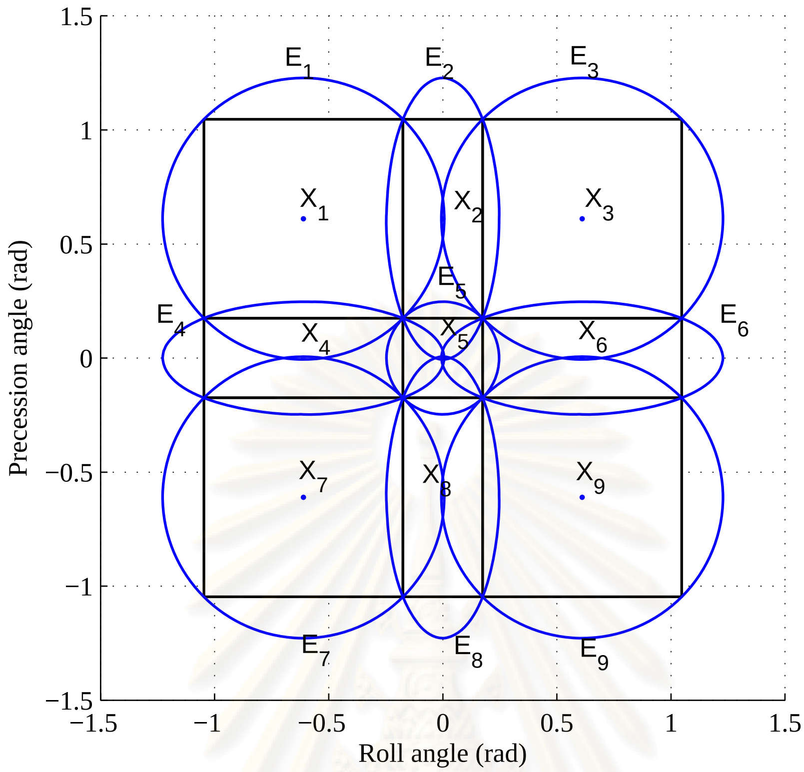

Figure 6.1: Polyhedral partition with its outer minimum volumn ellipsoid approximation.

The obtained gain L is used to feedback with $u = -Lx$ in the bicycle system. We show the simulation result of this control laws in the original nonlinear bicycle model (Figure 6.2) and the approximated PWA model (Figure 6.3).

From the series of resulting plots in Figures 6.4-6.11, we conclude that the gain L can perfectly stabilize the approximated PWA system and also the original nonlinear bicycle system. Moreover, the approximated PWA model yield a very good response as it travels quite close to the nonlinear trajectory for all partitioned regions.

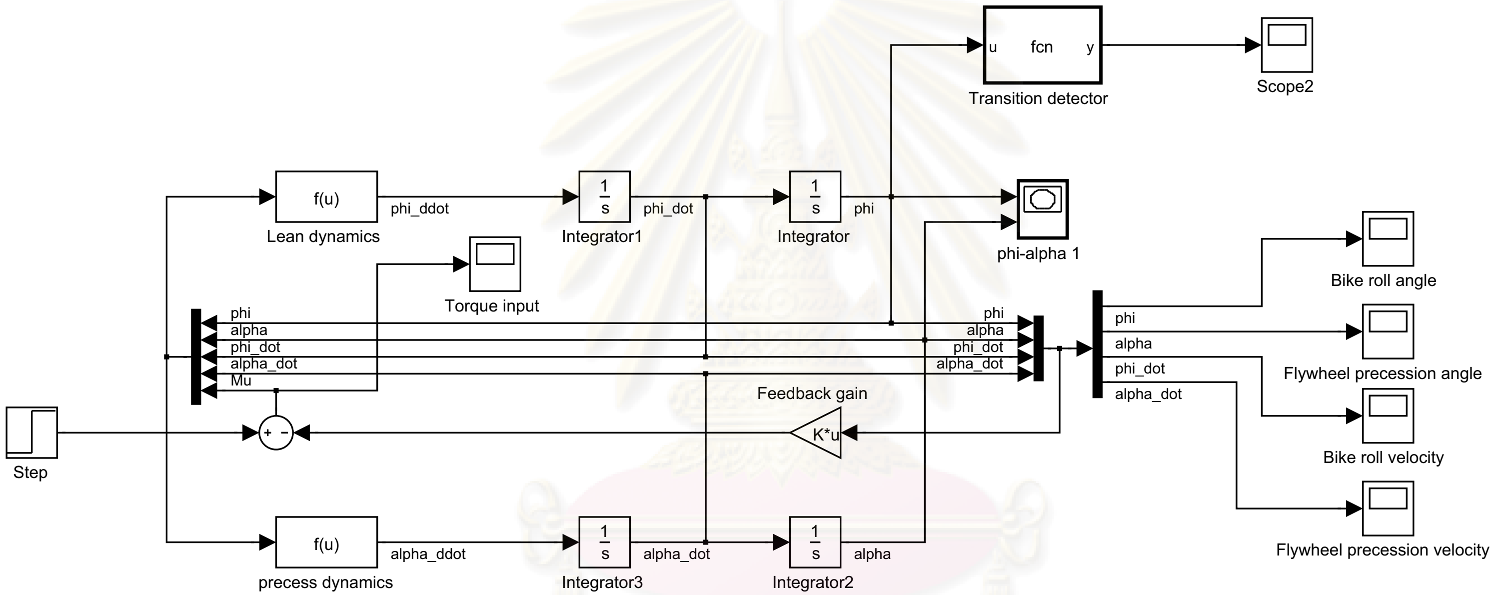

Figure 6.2: Simulink model of nonlinear bicycle model.

41

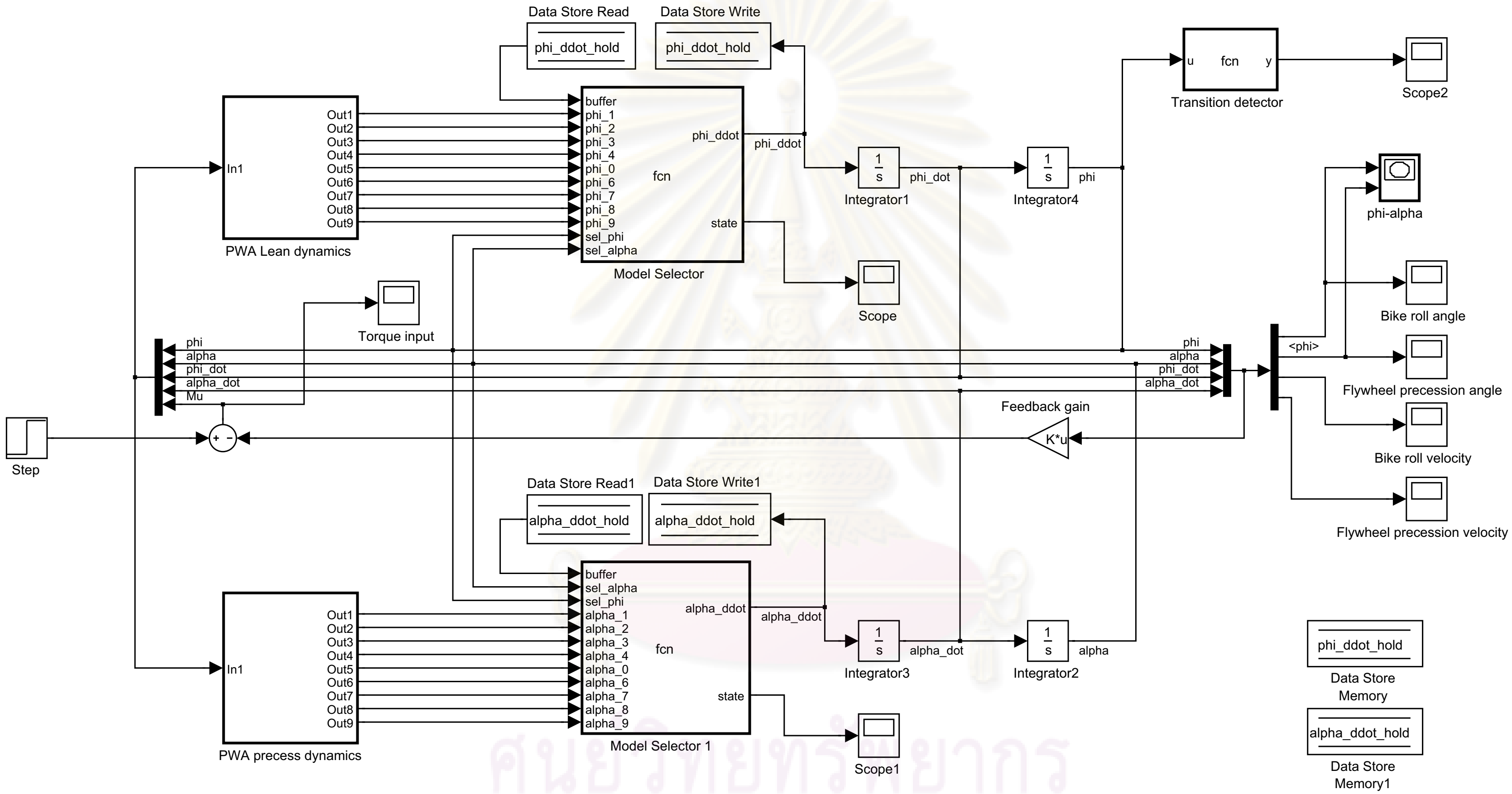

Figure 6.3: Simulink model - PWA bicycle model.

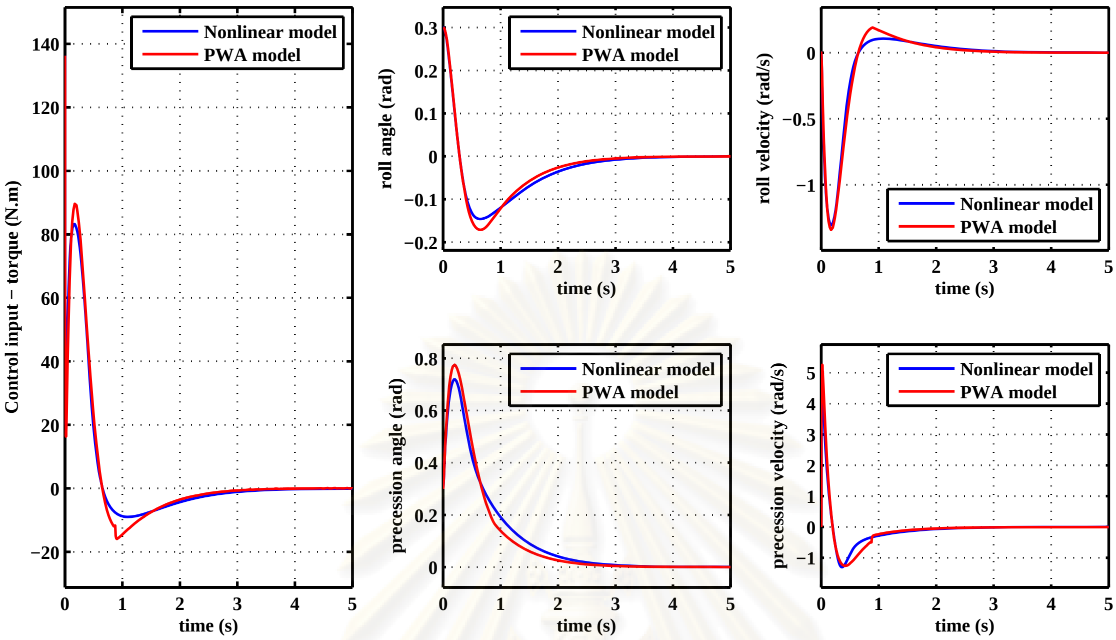

Figure 6.4: The response of roll angle, roll velocity, precession angle, and precession velocity of Nonlinear and PWA model with the initial condition $(\varphi(0), \alpha(0), \dot{\varphi}(0), \dot{\alpha}(0)) = (0.3, 0.3, 0, 0)$.

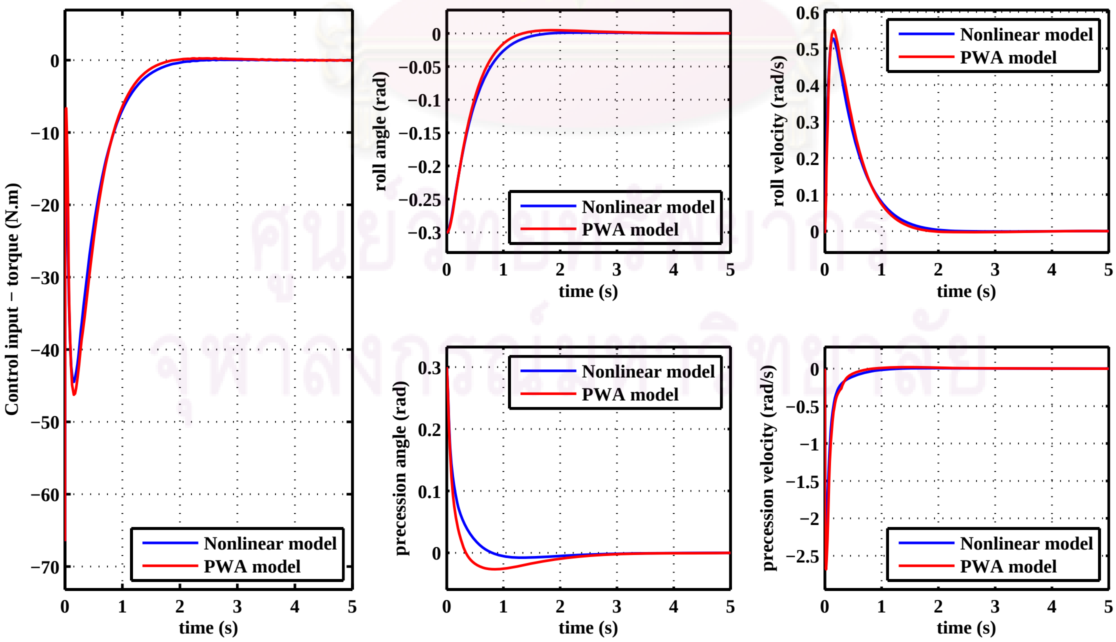

Figure 6.5: The response of roll angle, roll velocity, precession angle, and precession velocity of Nonlinear and PWA model with the initial condition $(\varphi(0), \alpha(0), \dot{\varphi}(0), \dot{\alpha}(0)) = (-0.3, 0.3, 0, 0)$.

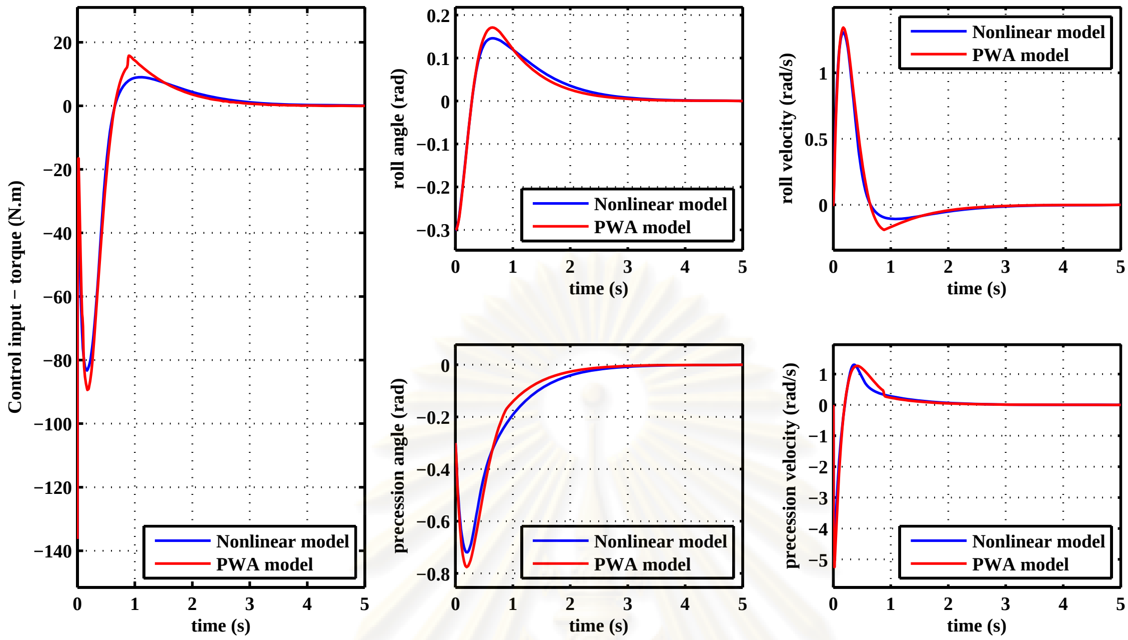

Figure 6.6: The response of roll angle, roll velocity, precession angle, and precession velocity of Nonlinear and PWA model with the initial condition $(\varphi(0), \alpha(0), \dot{\varphi}(0), \dot{\alpha}(0)) = (-0.3, -0.3, 0, 0)$.

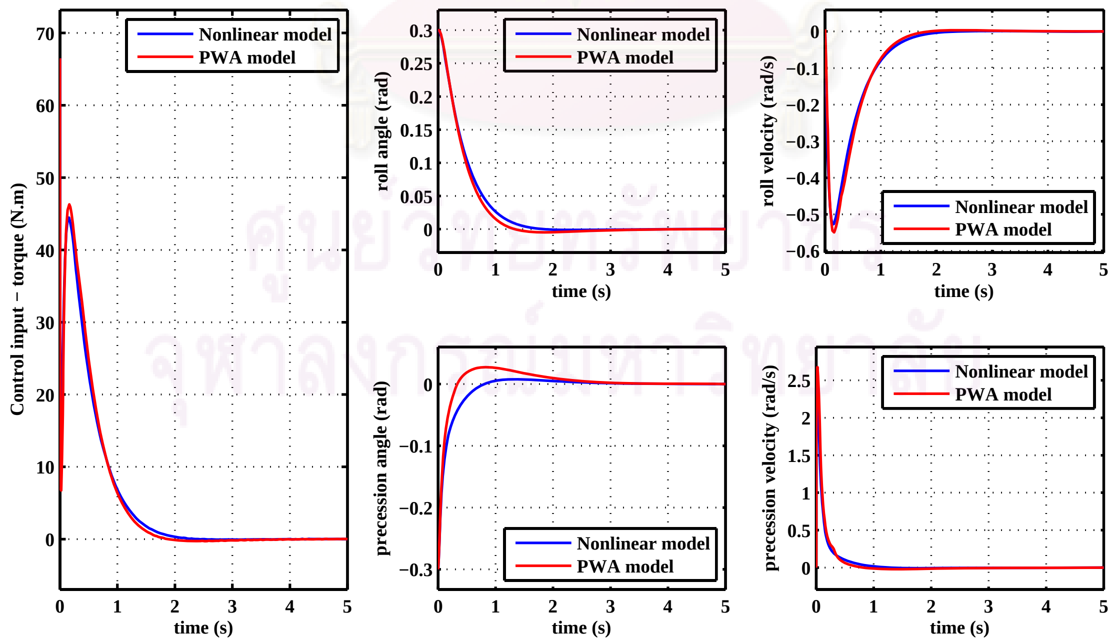

Figure 6.7: The response of roll angle, roll velocity, precession angle, and precession velocity of Nonlinear and PWA model with the initial condition $(\varphi(0), \alpha(0), \dot{\varphi}(0), \dot{\alpha}(0)) = (0.3, -0.3, 0, 0)$.

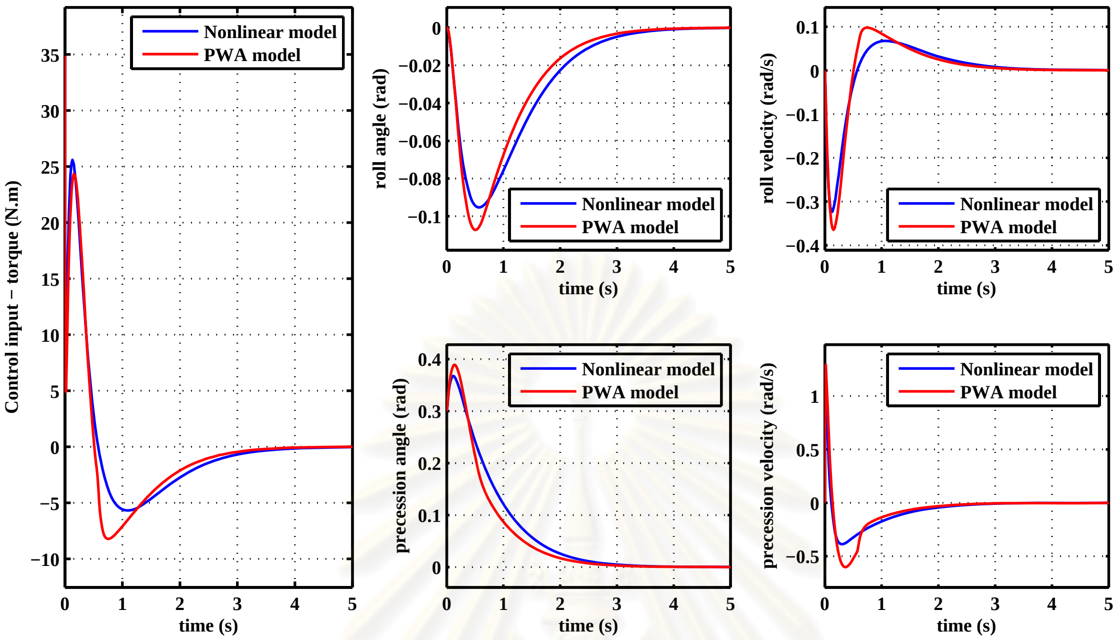

Figure 6.8: The response of roll angle, roll velocity, precession angle, and precession velocity of Nonlinear and PWA model with the initial condition $(\varphi(0), \alpha(0), \dot{\varphi}(0), \dot{\alpha}(0)) = (0, 0.3, 0, 0)$.

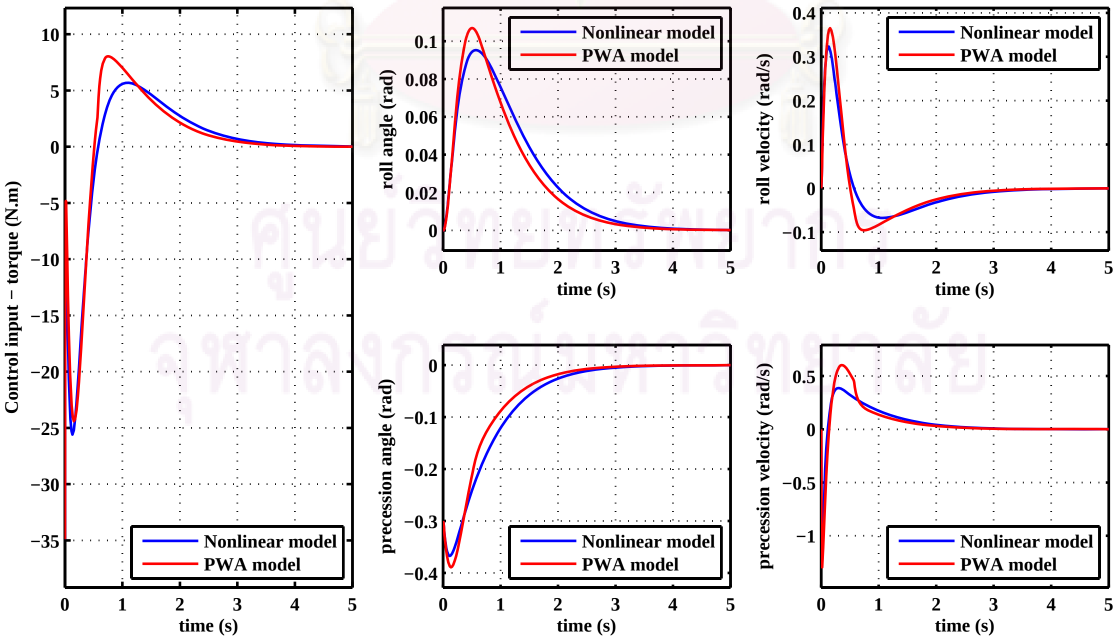

Figure 6.9: The response of roll angle, roll velocity, precession angle, and precession velocity of Nonlinear and PWA model with the initial condition $(\varphi(0), \alpha(0), \dot{\varphi}(0), \dot{\alpha}(0)) = (0, -0.3, 0, 0)$.

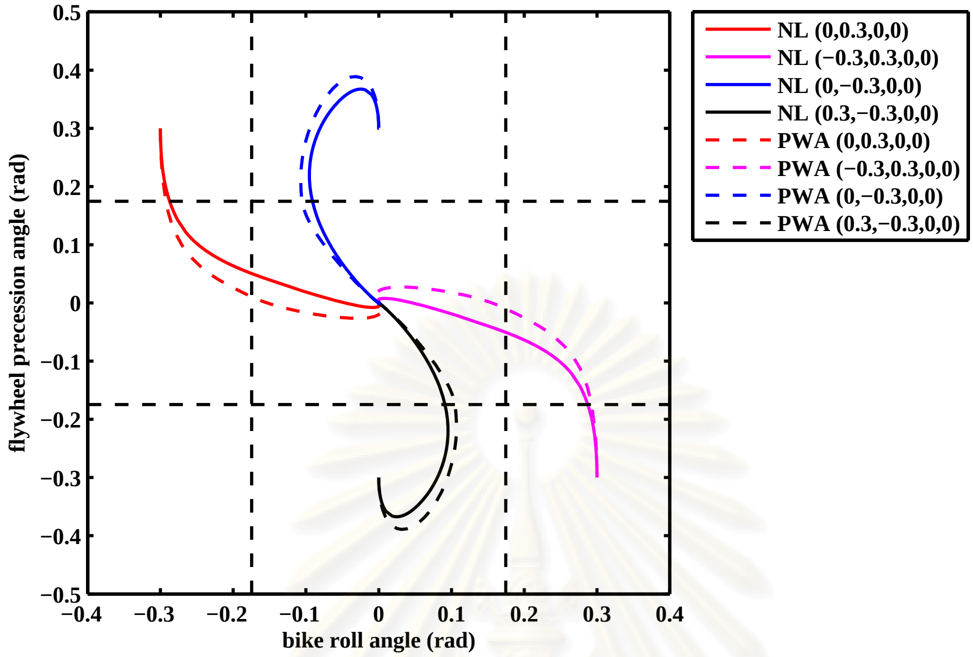

Figure 6.10: The trajectory of bike roll angle vs flywheel precession angle with 4 sets of initial conditions $(\varphi(0), \alpha(0), \dot{\varphi}(0), \dot{\alpha}(0))$.

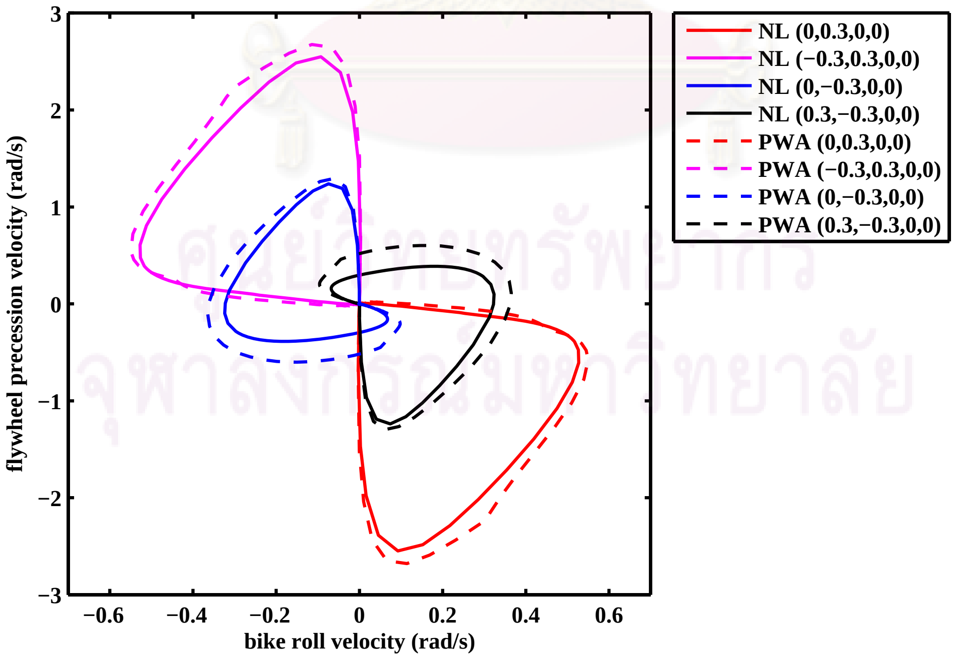

Figure 6.11: The trajectory of bike roll velocity vs flywheel precession velocity with 4 sets of initial conditions $(\varphi(0), \alpha(0), \dot{\varphi}(0), \dot{\alpha}(0))$.

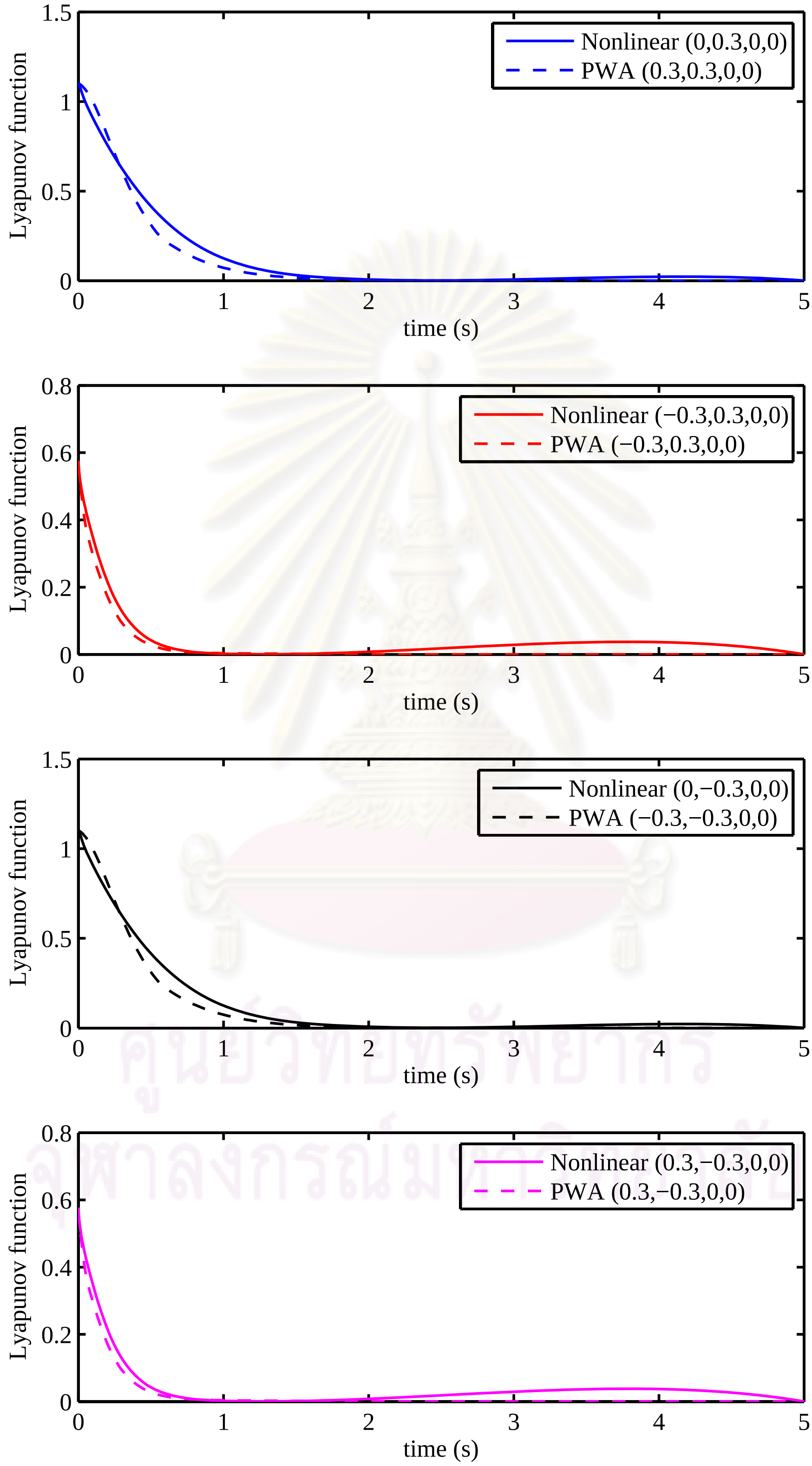

Figure 6.12: Lyapunov function plot of the bicycle dynamic system.

CHAPTER VII

CONCLUSIONS

7.1 Summary

This thesis has proposed the new idea of bicycle robot control using gyroscopic stabilization effect. This idea encounters the nonlinear unstable bicycle system by modeling it into a set of linear model or piecewise affine model. Then, the piecewise quadratic stability theorem can be applied and used for searching for the globally quadratic Lyapunov function to guarantee the system stability. Furthermore, this condition can be extended with the ellipsoid cell boundings to derive the feedback stabilization gain. The effectiveness of the proposed method has been illustrated through simulation examples. To summarize the thesis, we highlight main topics in the following.

Chapter 1 briefly introduces the motivation behind the research. Next, the literature review is given to cover an overview of bicycle model and its control method as well as some application of PWA systems. Afterward, we present the thesis objective, scope and research contributions.

In Chapter 2, a basic knowledge with some important concepts of a bicycle; its nature and the effect of gyroscopic which can help stabilize the bicycle. An important tool to be used to derive the dynamic equation of the bicycle are included in this chapter. The overview of PWA system and its representation of matrix parameterization has been introduced. And it follows with the quadratic stability condition that uses for finding the quadratic Lyapunov function and the feedback control gain. In chapter 3, the parameter measurement and calculation on the experimental bicycle are performed. The major apparatus are the body of the bicycle itself and the gyroscopic flywheel. Some parameters are obtained by the real measurement and some are obtained through the CAD modeling program based on the real bike parameters.

Chapter 4 and 5 presents the detail steps in deriving the nonlinear dynamic model of an autonomous bicycle using gyroscopic effect and an approximation of this model to be the PWA model. The nonlinear dynamic model is derived by Lagrangian mechanics theory. The PWA model is approximated by the 3 proposed methods, i.e. trigonometric terms approximation, Least-square error approximation without boundary constraints, and Least-square error approximation with boundary constraints.

Finally, all information from the former chapters are gathered to formulate the quadratic stabilization problem. The unconstrained was selected as a PWA model to solve for the feedback stabilization gain. The graphical results are also shown in various initial conditions accompanied with the comparison of the response of the nonlinear model and the approximated PWA model.

The conclusion and future work guideline are briefly described at the end.

7.2 Future Work Guideline

1. *Control of autonomous bicycle with bicycle velocity feedback*
   The result of bicycle control in this thesis starts from the simpler case which does not tackle the problem of bicycle speed varying. As we saw in Chapter 2 that the bicycle gives a significant effect on the bicycle stability, so it is expected to be easier to utilize the speed to help stabilize the bicycle. However, the problem will be more complex in the bicycle modeling and the mutual effect to the bicycle roll angle by the gyroscopic effect and bicycle velocity.

2. *PWA Identification of an autonomous bicycle using gyroscopic effect*
   There are another methods for deriving the PWA model of the bicycle. The PWA model proposed in this thesis is derived by a simple technique and thus easy to debug. We recommend to proceed to the more advance technique that has been studied widely in [54], [55], [42], [56], [57], [58], [59], [60] and in Ph.D. thesis [61].

3. *An implementation on the real bicycle*
   To the best proof of this control strategy, an implementation on the real hardware is encouraged. From the author experience, since there is no ready bicycle robot for testing the control laws in the market and an individual work is quite a large burden to be busy working on the electronics and mechanics stuff, this future work is recommended to be done in a team.

REFERENCES

[1] Wikipedia. Bicycle and motorcycle dynamics, [Online]. Available at http://en.wikipedia.org/wiki/Bicycle_and_motorcycle_dynamics [last modified on 9 July 2010 at 16:37].

[2] Spry, S. C., and Girard, A. R. Gyroscopic Stabilization of Unstable Vehicles: Configurations, Dynamics, and Control. March 2008. (Unpublished Manuscript)

[3] Johansson, M. Piecewise linear control systems: A computational approach. Germany: Springer-Verlag Berlin Heidelberg, 2003.

[4] Schwab, A., Meijaard, J., Ruine, A., and Papadopoulos, J. Linearized dynamics equations for the balance and steer of a bicycle. September 2007. (Unpublished Manuscript)

[5] Getz, N. Internal equilibrium control of a bicycle. in Proceedings of the 34th IEEE Conference on Decision and Control, vol. 4, pp. 4285–4287, December 1995.

[6] Getz, N., and Marsden, J. Control for an autonomous bicycle. in Proceedings of the IEEE International Conference on Robotics and Automation, vol. 2. May 1995.

[7] Getz, N. H. Dynamic Inversion of Nonlinear Maps with Applications to Nonlinear Control and Robotics, Doctoral dissertation, Department of Electrical Engineering and Computer Sciences University of California at Berkeley, CA, USA, 1999.

[8] Getz, N. Control of balance for a nonlinear nonholonomic non-minimum phase model of a bicycle. in Proceedings of the American Control Conference, vol. 1, pp. 148–151, June 1994.

[9] Yi, J., Song, D., Levandowski, A., and Jayasuriya, S. Trajectory tracking and balance stabilization control of autonomous motorcycles. in Proceedings of the IEEE International Conference on Robotics and Automation, pp. 2583–2589, May 2006.

[10] Defoort, M., and Murakami, T. Sliding-Mode Control Scheme for an Intelligent Bicycle. IEEE Transactions on Industrial Electronics, vol. 56, No. 9, pp. 3357–3368, September 2009.

[11] Chidzonga, R., and Chikuni, E. Stabilizing a bicycle below critical speed. in Proceedings of the African Conference, pp. 1–7, September 2007.

[12] Yamaguchi, T., Shibata, T., and Murakami, T. Self-Sustaining Approach of Electric Bicycle by Acceleration Control Based backstepping. in Proceedings of the 33rd Annual Conference of the IEEE Industrial Electronics Society, pp. 2610–2614, November 2007.

[13] Tanaka, Y. and Murakami, T. Self sustaining bicycle robot with steering controller. in Proceedings of the 8th IEEE International Workshop on Advanced Motion Control, pp. 197–197, March 2004.

[14] Franke, G., Suhr, W., and Rieß, F. An advanced model of bicycle dynamics. European Journal of Physics 11 (1990): 116–121.

[15] Åström, K., Klein, R., and Lennartsson, A. Bicycle dynamics and control: adapted bicycles for education and research. IEEE Control Systems Magazine 25 (August 2005): 26–47.

[16] Limebeer, D., and Sharp, R. Bicycles, motorcycles, and models. IEEE Control Systems Magazine 26 (October 2006): 34–61.

[17] Guo, L., Liao, Q., and Wei, S. Nonlinear stabilization of bicycle robot steering control system. in Proceedings of the International Conference on Mechatronics and Automation, pp. 3185–3189, August 2009.

[18] Guo, L., Liao, Q., Wei, Si, and Zhuang Yi. Design of linear quadratic optimal controller for bicycle robot. in Proceedings of the IEEE International Conference on Automation and Logistics, pp. 1968–1972, August 2009.

[19] Guo, L., Liao, Q., and Wei, S. Design of Fuzzy Sliding-mode Controller for Bicycle Robot Nonlinear System. in Proceedings of the IEEE International Conference on Robotics and Biomimetics, pp. 176–180, December 2006.

[20] Guo, L., Liao, Q., and Wei, S. Design of Motion Controller for Bicycle Robot Based on DFL Nonlinear Control Method. in Proceedings of the 6th World Congress on Intelligent Control and Automation, vol. 2, pp. 9047–9051, 2006.

[21] Schwab, A., Meijaard, J., and Papadopoulos, J. Benchmark results on the linearized equations of motion of an uncontrolled bicycle. Journal of Mechanical Science and Technology 19 (2005): 292–304.

[22] Yamakita, M., and Utano, A. Automatic control of bicycles with a balancer. in Proceedings of the IEEE/ASME International Conference on Advanced Intelligent Mechatronics, pp. 1245–1250, July 2005.

[23] Keo, L., and Yamakita, M. Controlling balancer and steering for bicycle stabilization. in Proceedings of the IEEE/RSJ International Conference on Intelligent Robots and Systems, pp.4541–4546, October 2009.

[24] Keo, L., and Yamakita, M. Controller design of an autonomous bicycle with both steering and balancer controls. in Proceedings of the IEEE Control Applications and Intelligent Control, pp. 1294–1299, July 2009.

[25] Thanh, T. B., and Parnichkun, M. Balancing Control of Bicyrobo by Particle Swarm Optimization-based Structure Specified Mixed H_2/H_∞ Control. International Journal of Advanced Robotic Systems 5 (2008): 315–326.

[26] Karnopp, D. Tilt Control for Gyro-Stabilized Two-Wheeled Vehicles. Vehicle System Dynamics 37 (2002): 145–156.

[27] Gallaspy, J. Gyroscopic stabilization of an unmanned bicycle. Master's thesis, Auburn University, 1999.

[28] Beznos, A., et. al. Control of autonomous motion of two-wheel bicycle with gyroscopic stabilisation. in Proceedings of the IEEE International Conference on Robotics and Automation, vol. 3, pp. 2670–2675, May 1998.

[29] Michini, B. Autonomous Stability Control of a Moving Bicycle 16.621 version III. Technical Report. MIT, Spring 2006.

[30] Kooijman, J. D. G. Experimental Validation of a Model for the Motion of an Uncontrolled Bicycle. Master's thesis, Delft University of Technology, Netherland, 2006.

[31] Julian, P., Desages, A., and Agamennoni, O. High-level canonical piecewise linear representation using a simplicial partition. IEEE Transactions on Circuits and Systems I: Fundamental Theory and Applications, vol. 46, no. 4, pp. 463–480, April 1999.

[32] Leenaerts, D. M. W., and Bokhoven, W. M. V. Piecewise Linear Modeling and Analysis. Norwell, MA, USA: Kluwer Academic Publishers, 1998.

[33] Chua, L., and Kang, S. M. Section-wise piecewise-linear functions: Canonical representation, properties, and applications. in Proceedings of the IEEE, vol. 65, no. 6, pp. 915–929, June 1977.

[34] Azuma, S., Imura, J., and Sugie, T. Lebesgue Piecewise Affine Approximation of Nonlinear Systems and Its Application to Hybrid System Modeling of Biosystems. in Proceedings of the 45th IEEE Conference on Decision and Control, pp. 2128–2133, December 2006.

[35] D'Ambrosio, C., Lodi, A., and Martello, S. Piecewise linear approximation of functions of two variables in MILP models. Operations Research Letters, 38 (2010): 39–46.

[36] Papadakis, S., and Kaburlasos, V. G. Piecewise-linear approximation of non-linear models based on probabilistically/possibilistically interpreted intervals' numbers (INs). Information Sciences 180 (2010): 5060–5076.

[37] Hassibi, A., and Boyd, S. Quadratic stabilization and control of piecewise-linear systems. in Proceedings of the 1998 American Control Conference, vol. 6, pp. 3659–3664, June 1998.

[38] Mignone, D., Ferrari-Trecate, G, and Morari, M. Stability and stabilization of piecewise affine and hybrid systems: an LMI approach. in Proceedings of the 39th IEEE Conference on Decision and Control, vol. 1, pp. 504–509, 2000.

[39] Rantzer, A., and Johansson, M. Piecewise linear quadratic optimal control. IEEE Transactions on Automatic Control 45 (April 2000): 629–637.

[40] Ferrari-Trecate, G., Muselli, M., Liberati, D., and Morari, M. Identification of piecewise affine and hybrid systems. in Proceedings of the American Control Conference, vol. 5, pp. 3521–3526, 2001.

[41] Bemporad, A., Garulli, A., Paoletti, S., and Vicino, A. A bounded-error approach to piecewise affine system identification. IEEE Transactions on Automatic Control 50 (October 2005): 1567–1580.

[42] Tabatabaei-Pour, M., Gholami, M., Salahshoor, K., and Shaker, H. A Clustering-Based Bounded-Error Approach for Identification of PWA Hybrid Systems. in Proceedings of the 9th International Conference on Control, Automation, Robotics and Vision, pp. 1–6, December 2006.

[43] Mulder, E., and Kothare, M. Synthesis of stabilizing anti-windup controllers using piecewise quadratic Lyapunov functions. in Proceedings of the 2000 American Control Conference, vol. 5, pp. 3239–3243, 2000.

[44] Keshavarz, M., Yazdi, M.B., and Jahed-Motlagh, M.R. Piecewise affine modeling and control of a boiler-turbine unit. Applied Thermal Engineering 30 (2010): 781–791.

[45] Wijaya, S. Robust constrained model predictive control for piecewise affine systems using saturated linear feedback controller. Master's thesis, Department of Electrical Engineering, Chulalongkorn University, Thailand, 2009.

[46] Benine-Neto, A., Scalzi, S., Netto, M., Mammar, S., and Pasillas-Lepine, W. Vehicle yaw rate control based on piecewise affine regions. in Proceedings of the IEEE Intelligent Vehicles Symposium, pp. 20–25, June 2010.

[47] Scalzi, S., Benine-Neto, A., Netto, M., Pasillas-Lepine, W., and Mammar, S. Active steering control based on piecewise affine regions. in Proceedings of the American Control Conference, pp. 5362–5367, July 2010.

[48] Jones, D. E. H. The stability of the bicycle. Physics Today(1970): 34–40. (Re-published September 2006, pp. 51–56).

[49] Wikipedia. Lagrangian mechanics, [Online]. Available at http://en.wikipedia.org/wiki/Lagrangian_mechanics [last modified on 30 September 2010 at 12:11].

[50] Jintanawan, T. Advanced Dynamics. The accompanying Book for 2103-617 Advanced Dynamics. Department of Mechanical Engineering Chulalongkorn University, 2005.

[51] Meriam, J., and Kraige, K. Engineering Mechanics volume 2 Dynamics Fifth Edition SI Version. USA: John Wiley & Sons Inc., 2003.

[52] Löfberg, J. YALMIP : A Toolbox for Modeling and Optimization in MATLAB. ETH, [Online], 2004. Available at http://control.ee.ethz.ch/ joloef/yalmip.php.

[53] Tütüncü, R. H., Toh, K. C., and Todd, M. J. SDPT3 – a Matlab software package for semidefinite programming. Optimization Methods and Software, vol. 11, pp. 545–581 , 1999.

[54] Bemporad, A, Roll, J., and Ljung, L. Identification of hybrid systems via mixed-integer programming. in Proceedings of the 40th IEEE Conference on Decision and Control, vol. 1, pp. 786–792, 2001.

[55] Ma, S., Zanma, T., and Ishida, M. Identification of switched systems with unknown switch points and its application. in Proceedings of the IEEE International Conference on Systems, Man and Cybernetics, vol. 3, pp. 2885–2890, October 2005.

[56] Tabatabaci-Pour, M., Gholami, M., Shaker, H., and Moshiri, B. Recursive Identification of Piecewise Affine Hybrid Systems. in Proceedings of the 9th International Conference on Control, Automation, Robotics and Vision, pp. 1–6, December 2006.

[57] Miyashita, N., and Yamakita, M. Identification of Hammerstein Systems with Piecewise-Affine Nonlinearities. in Proceedings of the American Control Conference, pp. 2265–2270, July 2007.

[58] Miyashita, N., and Yamakita, M. Identification of Hammerstein systems with piecewise nonlinearities with memory. in Proceedings of the 46th IEEE Conference on Decision and Control, pp.5749–5754, December 2007.

[59] Ferrari-Trecate, G., Muselli, M., Liberati, D., and Morari, M. Identification of piecewise affine and hybrid systems. in Proceedings of the American Control Conference, vol. 5, pp. 3521–3526 , 2001.

[60] Vidal, R. Identification of PWARX hybrid models with unknown and possibly different orders. in Proceedings of the American Control Conference, vol. 1, pp. 547–552, July 2004.

[61] Paoletti, S. Identification of piecewise affine models. Doctoral dissertation, Universita Degli Studi Di Siena, Italy, 2003.

APPENDICES

APPENDIX A

Constraint Matrices Formulation

The constraints matrices are the crucial parameters to define the region of the state in a polyhedral partition, to perform the PWA stability analysis and the controller synthesis. This section will show the summary how to construct the constraint matrices $\bar{G}_i, \bar{E}_i, \bar{F}_i, \bar{S}_i$. It is instructive to first formulate $\bar{H}$, $\bar{F}_i$, $\bar{G}_i$, and $\bar{E}_i$, respectively.

Polyhedral Hyperplane

From the definition of the hyperplane $\partial\mathcal{H}_k$ (2.9) and the hyperplane matrix $\bar{H}$ (2.10), it is obvious to obtain $\partial\mathcal{H}_k$ from the linear equation that separates any regions and all of them are collected in $\bar{H}$. Each hyperplane induced two closed half-spaces

$$\partial\mathcal{H}_k^+ = \{x \,|\, H_k x + h_k \geq 0\} \tag{1}$$

$$\partial\mathcal{H}_k^- = \{x \,|\, H_k x + h_k \leq 0\} \tag{2}$$

with the convention $h_k \leq 0$ that implies I_0 is always in $\partial\mathcal{H}_k^-$ for all $k \in K$.

Continuity Matrix

$$k\text{th row of } \bar{F}_i = \begin{cases} k\text{th row of } \bar{H}, & X_i \subseteq \partial\mathcal{H}_k^+ \\ \mathbf{0}, & \text{otherwise} \end{cases} \tag{3}$$

In order to make the continuity matrices full column rank, we can augment them according to

$$\bar{F}_i = \begin{bmatrix} F_i & f_i \\ I & 0 \end{bmatrix} \tag{4}$$

Cell Identifier

$$k\text{th row of } \bar{G}_i = \begin{cases} (-1) \times k\text{th row of } \bar{H}, & X_i \subseteq \partial\mathcal{H}_k^- \\ (+1) \times k\text{th row of } \bar{H}, & X_i \subseteq \partial\mathcal{H}_k^+ \end{cases}$$

Cell Bounding

The cell boundings $\bar{E}_i$ can be obtained by

- If $i \in I_0$, delete all rows of $\bar{G}_i$ whose the last entry is non-zero.
- If $i \in I_1$, and X_i is unbound, augment $\bar{G}_i$ with the row $\begin{bmatrix} 0_{1\times n} & 1 \end{bmatrix}$
- Otherwise, $\bar{E}_i = \bar{G}_i$.

The Constraint Matrices for PWA Bicycle model

Region	$\bar{G}_i$	$\bar{E}_i$	$\bar{F}_i$
X_1	$\begin{bmatrix} -1 & 0 & 0 & 0 & -0.1745 \\ 0 & 1 & 0 & 0 & -0.1745 \end{bmatrix}$	$\begin{bmatrix} -1 & 0 & 0 & 0 & -0.1745 \\ 0 & 1 & 0 & 0 & -0.1745 \\ 0 & 0 & 0 & 0 & 1 \\ 0 & 0 & 0 & 0 & 1 \end{bmatrix}$	$\begin{bmatrix} 0 & 0 & 0 & 0 & 0 \\ -1 & 0 & 0 & 0 & -0.1745 \\ 0 & 1 & 0 & 0 & -0.1745 \\ 0 & 0 & 0 & 0 & 0 \end{bmatrix}$
X_2	$\begin{bmatrix} -1 & 0 & 0 & 0 & 0.1745 \\ 1 & 0 & 0 & 0 & 0.1745 \\ 0 & 1 & 0 & 0 & -0.1745 \end{bmatrix}$	$\begin{bmatrix} -1 & 0 & 0 & 0 & 0.1745 \\ 1 & 0 & 0 & 0 & 0.1745 \\ 0 & 1 & 0 & 0 & -0.1745 \\ 0 & 0 & 0 & 0 & 1 \end{bmatrix}$	$\begin{bmatrix} 0 & 0 & 0 & 0 & 0 \\ 0 & 0 & 0 & 0 & 0 \\ 0 & 1 & 0 & 0 & -0.1745 \\ 0 & 0 & 0 & 0 & 0 \end{bmatrix}$
X_3	$\begin{bmatrix} 1 & 0 & 0 & 0 & -0.1745 \\ 0 & 1 & 0 & 0 & -0.1745 \end{bmatrix}$	$\begin{bmatrix} 1 & 0 & 0 & 0 & -0.1745 \\ 0 & 1 & 0 & 0 & -0.1745 \\ 0 & 0 & 0 & 0 & 1 \\ 0 & 0 & 0 & 0 & 1 \end{bmatrix}$	$\begin{bmatrix} 1 & 0 & 0 & 0 & -0.1745 \\ 0 & 0 & 0 & 0 & 0 \\ 0 & 1 & 0 & 0 & -0.1745 \\ 0 & 0 & 0 & 0 & 0 \end{bmatrix}$
X_4	$\begin{bmatrix} -1 & 0 & 0 & 0 & -0.1745 \\ 0 & -1 & 0 & 0 & 0.1745 \\ 0 & 1 & 0 & 0 & 0.1745 \end{bmatrix}$	$\begin{bmatrix} -1 & 0 & 0 & 0 & -0.1745 \\ 0 & -1 & 0 & 0 & 0.1745 \\ 0 & 1 & 0 & 0 & 0.1745 \\ 0 & 0 & 0 & 0 & 1 \end{bmatrix}$	$\begin{bmatrix} 0 & 0 & 0 & 0 & 0 \\ -1 & 0 & 0 & 0 & -0.1745 \\ 0 & 0 & 0 & 0 & 0 \\ 0 & 0 & 0 & 0 & 0 \end{bmatrix}$
X_5	$\begin{bmatrix} -1 & 0 & 0 & 0 & 0.1745 \\ 1 & 0 & 0 & 0 & 0.1745 \\ 0 & -1 & 0 & 0 & 0.1745 \\ 0 & 1 & 0 & 0 & 0.1745 \end{bmatrix}$	$\begin{bmatrix} 0 & 0 & 0 & 0 & 0 \\ 0 & 0 & 0 & 0 & 0 \\ 0 & 0 & 0 & 0 & 0 \\ 0 & 0 & 0 & 0 & 0 \end{bmatrix}$	$\begin{bmatrix} 0 & 0 & 0 & 0 & 0 \\ 0 & 0 & 0 & 0 & 0 \\ 0 & 0 & 0 & 0 & 0 \\ 0 & 0 & 0 & 0 & 0 \end{bmatrix}$
X_6	$\begin{bmatrix} 1 & 0 & 0 & 0 & -0.1745 \\ 0 & -1 & 0 & 0 & 0.1745 \\ 0 & 1 & 0 & 0 & 0.1745 \end{bmatrix}$	$\begin{bmatrix} 1 & 0 & 0 & 0 & -0.1745 \\ 0 & -1 & 0 & 0 & 0.1745 \\ 0 & 1 & 0 & 0 & 0.1745 \\ 0 & 0 & 0 & 0 & 1 \end{bmatrix}$	$\begin{bmatrix} 1 & 0 & 0 & 0 & -0.1745 \\ 0 & 0 & 0 & 0 & 0 \\ 0 & 0 & 0 & 0 & 0 \\ 0 & 0 & 0 & 0 & 0 \end{bmatrix}$
X_7	$\begin{bmatrix} -1 & 0 & 0 & 0 & -0.1745 \\ 0 & -1 & 0 & 0 & -0.1745 \end{bmatrix}$	$\begin{bmatrix} -1 & 0 & 0 & 0 & -0.1745 \\ 0 & -1 & 0 & 0 & -0.1745 \\ 0 & 0 & 0 & 0 & 1 \\ 0 & 0 & 0 & 0 & 1 \end{bmatrix}$	$\begin{bmatrix} 0 & 0 & 0 & 0 & 0 \\ -1 & 0 & 0 & 0 & -0.1745 \\ 0 & 0 & 0 & 0 & 0 \\ 0 & -1 & 0 & 0 & -0.1745 \end{bmatrix}$
X_8	$\begin{bmatrix} -1 & 0 & 0 & 0 & 0.1745 \\ 1 & 0 & 0 & 0 & 0.1745 \\ 0 & -1 & 0 & 0 & -0.1745 \end{bmatrix}$	$\begin{bmatrix} -1 & 0 & 0 & 0 & 0.1745 \\ 1 & 0 & 0 & 0 & 0.1745 \\ 0 & -1 & 0 & 0 & -0.1745 \\ 0 & 0 & 0 & 0 & 1 \end{bmatrix}$	$\begin{bmatrix} 0 & 0 & 0 & 0 & 0 \\ 0 & 0 & 0 & 0 & 0 \\ 0 & 0 & 0 & 0 & 0 \\ 0 & -1 & 0 & 0 & -0.1745 \end{bmatrix}$
X_9	$\begin{bmatrix} 1 & 0 & 0 & 0 & -0.1745 \\ 0 & -1 & 0 & 0 & -0.1745 \end{bmatrix}$	$\begin{bmatrix} 1 & 0 & 0 & 0 & -0.1745 \\ 0 & -1 & 0 & 0 & -0.1745 \\ 0 & 0 & 0 & 0 & 1 \\ 0 & 0 & 0 & 0 & 1 \end{bmatrix}$	$\begin{bmatrix} 1 & 0 & 0 & 0 & -0.1745 \\ 0 & 0 & 0 & 0 & 0 \\ 0 & 0 & 0 & 0 & 0 \\ 0 & -1 & 0 & 0 & -0.1745 \end{bmatrix}$

APPENDIX B

Ellipsoid Cell Boundings

In mathematics, the ellipsoid can be written in different ways, e.g. the quadratic set, the shape matrix with uncertainty, etc. We will not go further to those topics. The minimum volume ellipsoid that cover each polyhedral cell in this thesis is suitable to define in this form

$$\mathcal{E}_{mve} = \{x \in \mathbb{R}^n \mid \|Sx + s\|_2 \leq 1\}$$

Our interested parameter of polyhedral cell is its m vertices v_i. The minimum volume ellipsoid is obtained by solving the following convex optimization problem

$$\begin{array}{ll} \text{minimize} & \log\det S^{-1} \\ \text{subject to} & \begin{bmatrix} I & Sv_i + s \\ v_i^T S^T + s^T & 1 \end{bmatrix} \geq 0, \quad i = 1, \ldots, m \\ & S = S^T > 0 \end{array} \tag{5}$$

We call S an ellipsoid cell bounding. It is useful for deriving the control law as shown in Theorem 2.2.

The Ellipsoid Cell Bounding for PWA Bicycle model

The computed parameter, polyhedral vertices, and the resulted ellipsoid cell bounding in all 9 regions are listed below.

$$\begin{array}{lll} x_a = 0.1745 & y_a = 0.1745 & z_a = 100 \\ x_b = 1.0472 & y_b = 1.0472 & z_b = 100 \end{array}$$

x_a and x_b denote the bounding point of parameter φ $(10°, 60°)$.
y_a and y_b denote the bounding point of parameter α $(10°, 60°)$.
z_b denotes the bounding point of parameter $\dot{\varphi}, \dot{\alpha}$ (no bounding, so we assign a sufficiently high value).

<u>Polytope X_1</u>

$$v^1_{11} = \begin{bmatrix} -x_a \\ y_b \\ -z_b \\ -z_b \end{bmatrix} \quad v^1_{12} = \begin{bmatrix} -x_a \\ y_b \\ -z_b \\ z_b \end{bmatrix} \quad v^1_{13} = \begin{bmatrix} -x_a \\ y_b \\ z_b \\ -z_b \end{bmatrix} \quad v^1_{14} = \begin{bmatrix} -x_a \\ y_b \\ z_b \\ z_b \end{bmatrix}$$

$$v^1_{21} = \begin{bmatrix} -x_b \\ y_b \\ -z_b \\ -z_b \end{bmatrix} \quad v^1_{22} = \begin{bmatrix} -x_b \\ y_b \\ -z_b \\ z_b \end{bmatrix} \quad v^1_{23} = \begin{bmatrix} -x_b \\ y_b \\ z_b \\ -z_b \end{bmatrix} \quad v^1_{24} = \begin{bmatrix} -x_b \\ y_b \\ z_b \\ z_b \end{bmatrix}$$

$$v^1_{31} = \begin{bmatrix} -x_b \\ y_a \\ -z_b \\ -z_b \end{bmatrix} \quad v^1_{32} = \begin{bmatrix} -x_b \\ y_a \\ -z_b \\ z_b \end{bmatrix} \quad v^1_{33} = \begin{bmatrix} -x_b \\ y_a \\ z_b \\ -z_b \end{bmatrix} \quad v^1_{34} = \begin{bmatrix} -x_b \\ y_a \\ z_b \\ z_b \end{bmatrix}$$

$$v^1_{41} = \begin{bmatrix} -x_a \\ y_a \\ -z_b \\ -z_b \end{bmatrix} \quad v^1_{42} = \begin{bmatrix} -x_a \\ y_a \\ -z_b \\ z_b \end{bmatrix} \quad v^1_{43} = \begin{bmatrix} -x_a \\ y_a \\ z_b \\ -z_b \end{bmatrix} \quad v^1_{44} = \begin{bmatrix} -x_a \\ y_a \\ z_b \\ z_b \end{bmatrix}$$

<u>Ellipsoid $\mathcal{E}_1$</u>

$$S_1 = \begin{bmatrix} 1.1459 & 0 & 0 & 0 \\ 0 & 1.1459 & 0 & 0 \\ 0 & 0 & 0.0050 & 0 \\ 0 & 0 & 0 & 0.0050 \end{bmatrix} \qquad s_1 = \begin{bmatrix} 0.7 \\ -0.7 \\ 0 \\ 0 \end{bmatrix}$$

<u>Polytope X_2</u>

$$v^2_{11} = \begin{bmatrix} x_a \\ y_b \\ -z_b \\ -z_b \end{bmatrix} \quad v^2_{12} = \begin{bmatrix} x_a \\ y_b \\ -z_b \\ z_b \end{bmatrix} \quad v^2_{13} = \begin{bmatrix} x_a \\ y_b \\ z_b \\ -z_b \end{bmatrix} \quad v^2_{14} = \begin{bmatrix} x_a \\ y_b \\ z_b \\ z_b \end{bmatrix}$$

$$v^2_{21} = \begin{bmatrix} -x_a \\ y_b \\ -z_b \\ -z_b \end{bmatrix} \quad v^2_{22} = \begin{bmatrix} -x_a \\ y_b \\ -z_b \\ z_b \end{bmatrix} \quad v^2_{23} = \begin{bmatrix} -x_a \\ y_b \\ z_b \\ -z_b \end{bmatrix} \quad v^2_{24} = \begin{bmatrix} -x_a \\ y_b \\ z_b \\ z_b \end{bmatrix}$$

$$v^2_{31} = \begin{bmatrix} -x_a \\ y_a \\ -z_b \\ -z_b \end{bmatrix} \quad v^2_{32} = \begin{bmatrix} -x_a \\ y_a \\ -z_b \\ z_b \end{bmatrix} \quad v^2_{33} = \begin{bmatrix} -x_a \\ y_a \\ z_b \\ -z_b \end{bmatrix} \quad v^2_{34} = \begin{bmatrix} -x_a \\ y_a \\ z_b \\ z_b \end{bmatrix}$$

$$v^2_{41} = \begin{bmatrix} x_a \\ y_a \\ -z_b \\ -z_b \end{bmatrix} \quad v^2_{42} = \begin{bmatrix} x_a \\ y_a \\ -z_b \\ z_b \end{bmatrix} \quad v^2_{43} = \begin{bmatrix} x_a \\ y_a \\ z_b \\ -z_b \end{bmatrix} \quad v^2_{44} = \begin{bmatrix} x_a \\ y_a \\ z_b \\ z_b \end{bmatrix}$$

<u>Ellipsoid $\mathcal{E}_2$</u>

$$S_2 = \begin{bmatrix} 2.8647 & 0 & 0 & 0 \\ 0 & 1.1459 & 0 & 0 \\ 0 & 0 & 0.0050 & 0 \\ 0 & 0 & 0 & 0.0050 \end{bmatrix} \qquad s_2‘ = \begin{bmatrix} 0 \\ -0.7 \\ 0 \\ 0 \end{bmatrix}$$

Polytope X_3

$$v_{11}^3 = \begin{bmatrix} x_b \\ y_b \\ -z_b \\ -z_b \end{bmatrix} \quad v_{12}^3 = \begin{bmatrix} x_b \\ y_b \\ -z_b \\ z_b \end{bmatrix} \quad v_{13}^3 = \begin{bmatrix} x_b \\ y_b \\ z_b \\ -z_b \end{bmatrix} \quad v_{14}^3 = \begin{bmatrix} x_b \\ y_b \\ z_b \\ z_b \end{bmatrix}$$

$$v_{21}^3 = \begin{bmatrix} -x_a \\ y_b \\ -z_b \\ -z_b \end{bmatrix} \quad v_{22}^3 = \begin{bmatrix} -x_a \\ y_b \\ -z_b \\ z_b \end{bmatrix} \quad v_{23}^3 = \begin{bmatrix} -x_a \\ y_b \\ z_b \\ -z_b \end{bmatrix} \quad v_{24}^3 = \begin{bmatrix} -x_a \\ y_b \\ z_b \\ z_b \end{bmatrix}$$

$$v_{31}^3 = \begin{bmatrix} -x_a \\ y_a \\ -z_b \\ -z_b \end{bmatrix} \quad v_{32}^3 = \begin{bmatrix} -x_a \\ y_a \\ -z_b \\ z_b \end{bmatrix} \quad v_{33}^3 = \begin{bmatrix} -x_a \\ y_a \\ z_b \\ -z_b \end{bmatrix} \quad v_{34}^3 = \begin{bmatrix} -x_a \\ y_a \\ z_b \\ z_b \end{bmatrix}$$

$$v_{41}^3 = \begin{bmatrix} x_b \\ y_a \\ -z_b \\ -z_b \end{bmatrix} \quad v_{42}^3 = \begin{bmatrix} x_b \\ y_a \\ -z_b \\ z_b \end{bmatrix} \quad v_{43}^3 = \begin{bmatrix} x_b \\ y_a \\ z_b \\ -z_b \end{bmatrix} \quad v_{44}^3 = \begin{bmatrix} x_b \\ y_a \\ z_b \\ z_b \end{bmatrix}$$

Ellipsoid $\mathcal{E}_3$

$$S_3 = \begin{bmatrix} 1.1459 & 0 & 0 & 0 \\ 0 & 1.1459 & 0 & 0 \\ 0 & 0 & 0.0050 & 0 \\ 0 & 0 & 0 & 0.0050 \end{bmatrix} \quad s_3 = \begin{bmatrix} -0.7 \\ -0.7 \\ 0 \\ 0 \end{bmatrix}$$

Polytope X_4

$$v_{11}^4 = \begin{bmatrix} -x_a \\ y_a \\ -z_b \\ -z_b \end{bmatrix} \quad v_{12}^4 = \begin{bmatrix} -x_a \\ y_a \\ -z_b \\ z_b \end{bmatrix} \quad v_{13}^4 = \begin{bmatrix} -x_a \\ y_a \\ z_b \\ -z_b \end{bmatrix} \quad v_{14}^4 = \begin{bmatrix} -x_a \\ y_a \\ z_b \\ z_b \end{bmatrix}$$

$$v_{21}^4 = \begin{bmatrix} -x_b \\ y_a \\ -z_b \\ -z_b \end{bmatrix} \quad v_{22}^4 = \begin{bmatrix} -x_b \\ y_a \\ -z_b \\ z_b \end{bmatrix} \quad v_{23}^4 = \begin{bmatrix} -x_b \\ y_a \\ z_b \\ -z_b \end{bmatrix} \quad v_{24}^4 = \begin{bmatrix} -x_b \\ -y_a \\ z_b \\ z_b \end{bmatrix}$$

$$v_{31}^4 = \begin{bmatrix} -x_b \\ -y_a \\ -z_b \\ -z_b \end{bmatrix} \quad v_{32}^4 = \begin{bmatrix} -x_b \\ -y_a \\ -z_b \\ z_b \end{bmatrix} \quad v_{33}^4 = \begin{bmatrix} -x_b \\ -y_a \\ z_b \\ -z_b \end{bmatrix} \quad v_{34}^4 = \begin{bmatrix} -x_b \\ -y_a \\ z_b \\ z_b \end{bmatrix}$$

$$v_{41}^4 = \begin{bmatrix} -x_a \\ -y_a \\ -z_b \\ -z_b \end{bmatrix} \quad v_{42}^4 = \begin{bmatrix} -x_a \\ -y_a \\ -z_b \\ z_b \end{bmatrix} \quad v_{43}^4 = \begin{bmatrix} -x_a \\ -y_a \\ z_b \\ -z_b \end{bmatrix} \quad v_{44}^4 = \begin{bmatrix} -x_a \\ -y_a \\ z_b \\ z_b \end{bmatrix}$$

Ellipsoid $\mathcal{E}_4$

$$S_4 = \begin{bmatrix} 1.1459 & 0 & 0 & 0 \\ 0 & 2.8647 & 0 & 0 \\ 0 & 0 & 0.0050 & 0 \\ 0 & 0 & 0 & 0.0050 \end{bmatrix} \quad s_4 = \begin{bmatrix} 0.7 \\ 0 \\ 0 \\ 0 \end{bmatrix}$$

Polytope X_5

$$v_{11}^5 = \begin{bmatrix} x_a \\ y_a \\ -z_b \\ -z_b \end{bmatrix} \quad v_{12}^5 = \begin{bmatrix} x_a \\ y_a \\ -z_b \\ z_b \end{bmatrix} \quad v_{13}^5 = \begin{bmatrix} x_a \\ y_a \\ z_b \\ -z_b \end{bmatrix} \quad v_{14}^5 = \begin{bmatrix} x_a \\ y_a \\ z_b \\ z_b \end{bmatrix}$$

$$v_{21}^5 = \begin{bmatrix} -x_a \\ y_a \\ -z_b \\ -z_b \end{bmatrix} \quad v_{22}^5 = \begin{bmatrix} -x_a \\ y_a \\ -z_b \\ z_b \end{bmatrix} \quad v_{23}^5 = \begin{bmatrix} -x_a \\ y_a \\ z_b \\ -z_b \end{bmatrix} \quad v_{24}^5 = \begin{bmatrix} -x_a \\ y_a \\ z_b \\ z_b \end{bmatrix}$$

$$v_{31}^5 = \begin{bmatrix} -x_a \\ -y_a \\ -z_b \\ -z_b \end{bmatrix} \quad v_{32}^5 = \begin{bmatrix} -x_a \\ -y_a \\ -z_b \\ z_b \end{bmatrix} \quad v_{33}^5 = \begin{bmatrix} -x_a \\ -y_a \\ z_b \\ -z_b \end{bmatrix} \quad v_{34}^5 = \begin{bmatrix} x_a \\ -y_a \\ z_b \\ z_b \end{bmatrix}$$

$$v_{41}^5 = \begin{bmatrix} x_a \\ -y_a \\ -z_b \\ -z_b \end{bmatrix} \quad v_{42}^5 = \begin{bmatrix} x_a \\ -y_a \\ -z_b \\ z_b \end{bmatrix} \quad v_{43}^5 = \begin{bmatrix} x_a \\ -y_a \\ z_b \\ -z_b \end{bmatrix} \quad v_{44}^5 = \begin{bmatrix} x_a \\ -y_a \\ z_b \\ z_b \end{bmatrix}$$

Ellipsoid $\mathcal{E}_5$

$$S_5 = \begin{bmatrix} 2.8648 & 0 & 0 & 0 \\ 0 & 2.8648 & 0 & 0 \\ 0 & 0 & 0.0050 & 0 \\ 0 & 0 & 0 & 0.0050 \end{bmatrix} \quad s_5 = \begin{bmatrix} 0 \\ 0 \\ 0 \\ 0 \end{bmatrix}$$

Polytope X_6

$$v_{11}^6 = \begin{bmatrix} x_b \\ y_a \\ -z_b \\ -z_b \end{bmatrix} \quad v_{12}^6 = \begin{bmatrix} x_b \\ y_a \\ -z_b \\ -z_b \end{bmatrix} \quad v_{13}^6 = \begin{bmatrix} x_b \\ y_a \\ -z_b \\ -z_b \end{bmatrix} \quad v_{14}^6 = \begin{bmatrix} x_b \\ y_a \\ -z_b \\ -z_b \end{bmatrix}$$

$$v_{21}^6 = \begin{bmatrix} x_a \\ y_a \\ -z_b \\ z_b \end{bmatrix} \quad v_{22}^6 = \begin{bmatrix} x_a \\ y_a \\ z_b \\ -z_b \end{bmatrix} \quad v_{23}^6 = \begin{bmatrix} x_a \\ y_a \\ z_b \\ -z_b \end{bmatrix} \quad v_{24}^6 = \begin{bmatrix} x_a \\ y_a \\ z_b \\ -z_b \end{bmatrix}$$

$$v_{31}^6 = \begin{bmatrix} x_a \\ -y_a \\ z_b \\ -z_b \end{bmatrix} \quad v_{32}^6 = \begin{bmatrix} x_a \\ -y_a \\ -z_b \\ z_b \end{bmatrix} \quad v_{33}^6 = \begin{bmatrix} x_a \\ -y_a \\ -z_b \\ z_b \end{bmatrix} \quad v_{34}^6 = \begin{bmatrix} x_a \\ -y_a \\ -z_b \\ z_b \end{bmatrix}$$

$$v_{41}^6 = \begin{bmatrix} x_b \\ -y_a \\ z_b \\ z_b \end{bmatrix} \quad v_{42}^6 = \begin{bmatrix} x_b \\ -y_a \\ z_b \\ z_b \end{bmatrix} \quad v_{43}^6 = \begin{bmatrix} x_b \\ -y_a \\ z_b \\ z_b \end{bmatrix} \quad v_{44}^6 = \begin{bmatrix} x_b \\ -y_a \\ z_b \\ z_b \end{bmatrix}$$

Ellipsoid $\mathcal{E}_6$

$$S_6 = \begin{bmatrix} 1.1459 & 0 & 0 & 0 \\ 0 & 2.8647 & 0 & 0 \\ 0 & 0 & 0.0050 & 0 \\ 0 & 0 & 0 & 0.0050 \end{bmatrix} \quad s_6 = \begin{bmatrix} -0.7 \\ 0 \\ 0 \\ 0 \end{bmatrix}$$

Polytope X_7

$$v^{7}_{11} = \begin{bmatrix} -x_a \\ -y_a \\ -z_b \\ -z_b \end{bmatrix} \quad v^{7}_{12} = \begin{bmatrix} -x_a \\ -y_a \\ -z_b \\ z_b \end{bmatrix} \quad v^{7}_{13} = \begin{bmatrix} -x_a \\ -y_a \\ z_b \\ -z_b \end{bmatrix} \quad v^{=}_{14} \begin{bmatrix} -x_a \\ -y_a \\ z_b \\ z_b \end{bmatrix}$$

$$v^{7}_{21} = \begin{bmatrix} -x_b \\ -y_a \\ -z_b \\ -z_b \end{bmatrix} \quad v^{7}_{22} = \begin{bmatrix} -x_b \\ -y_a \\ -z_b \\ z_b \end{bmatrix} \quad v^{7}_{23} = \begin{bmatrix} -x_b \\ -y_a \\ z_b \\ -z_b \end{bmatrix} \quad v^{7}_{24} = \begin{bmatrix} -x_b \\ -y_a \\ z_b \\ z_b \end{bmatrix}$$

$$v^{7}_{31} = \begin{bmatrix} -x_b \\ -y_b \\ -z_b \\ -z_b \end{bmatrix} \quad v^{7}_{32} = \begin{bmatrix} -x_b \\ -y_b \\ -z_b \\ z_b \end{bmatrix} \quad v^{7}_{33} = \begin{bmatrix} -x_b \\ -y_b \\ z_b \\ -z_b \end{bmatrix} \quad v^{7}_{34} = \begin{bmatrix} -x_b \\ -y_b \\ z_b \\ z_b \end{bmatrix}$$

$$v^{7}_{41} = \begin{bmatrix} -x_a \\ -y_b \\ -z_b \\ -z_b \end{bmatrix} \quad v^{7}_{42} = \begin{bmatrix} -x_a \\ -y_b \\ -z_b \\ z_b \end{bmatrix} \quad v^{7}_{43} = \begin{bmatrix} -x_a \\ -y_b \\ z_b \\ -z_b \end{bmatrix} \quad v^{7}_{44} = \begin{bmatrix} -x_a \\ -y_b \\ z_b \\ z_b \end{bmatrix}$$

Ellipsoid $\mathcal{E}_7$

$$S_7 = \begin{bmatrix} 1.1459 & 0 & 0 & 0 \\ 0 & 1.1459 & 0 & 0 \\ 0 & 0 & 0.0050 & 0 \\ 0 & 0 & 0 & 0.0050 \end{bmatrix} \quad s_7 = \begin{bmatrix} 0.7 \\ 0.7 \\ 0 \\ 0 \end{bmatrix}$$

Polytope X_8

$$v^{8}_{11} = \begin{bmatrix} x_a \\ -y_a \\ -z_b \\ -z_b \end{bmatrix} \quad v^{8}_{12} = \begin{bmatrix} x_a \\ -y_a \\ -z_b \\ -z_b \end{bmatrix} \quad v^{8}_{13} = \begin{bmatrix} x_a \\ -y_a \\ -z_b \\ -z_b \end{bmatrix} \quad v^{8}_{14} = \begin{bmatrix} x_a \\ -y_a \\ -z_b \\ -z_b \end{bmatrix}$$

$$v^{8}_{21} = \begin{bmatrix} -x_a \\ -y_a \\ -z_b \\ z_b \end{bmatrix} \quad v^{8}_{22} = \begin{bmatrix} -x_a \\ -y_a \\ z_b \\ -z_b \end{bmatrix} \quad v^{8}_{23} = \begin{bmatrix} -x_a \\ -y_a \\ z_b \\ -z_b \end{bmatrix} \quad v^{8}_{24} = \begin{bmatrix} -x_a \\ -y_a \\ z_b \\ -z_b \end{bmatrix}$$

$$v^{8}_{31} = \begin{bmatrix} -x_a \\ -y_b \\ z_b \\ -z_b \end{bmatrix} \quad v^{8}_{32} = \begin{bmatrix} -x_a \\ -y_b \\ -z_b \\ z_b \end{bmatrix} \quad v^{8}_{33} = \begin{bmatrix} -x_a \\ -y_b \\ -z_b \\ z_b \end{bmatrix} \quad v^{8}_{34} = \begin{bmatrix} -x_a \\ -y_b \\ -z_b \\ z_b \end{bmatrix}$$

$$v^{8}_{41} = \begin{bmatrix} x_a \\ -y_b \\ z_b \\ z_b \end{bmatrix} \quad v^{8}_{42} = \begin{bmatrix} x_a \\ -y_b \\ z_b \\ z_b \end{bmatrix} \quad v^{8}_{43} = \begin{bmatrix} x_a \\ -y_b \\ z_b \\ z_b \end{bmatrix} \quad v^{8}_{44} = \begin{bmatrix} x_a \\ -y_b \\ z_b \\ z_b \end{bmatrix}$$

Ellipsoid $\mathcal{E}_8$

$$S_8 = \begin{bmatrix} 2.8647 & 0 & 0 & 0 \\ 0 & 1.1459 & 0 & 0 \\ 0 & 0 & 0.0050 & 0 \\ 0 & 0 & 0 & 0.0050 \end{bmatrix} \quad s_8 = \begin{bmatrix} 0 \\ 0.7 \\ 0 \\ 0 \end{bmatrix}$$

<u>Polytope X_9</u>

$$v_{11}^9 = \begin{bmatrix} x_b \\ -y_a \\ -z_b \\ -z_b \end{bmatrix} \quad v_{12}^9 = \begin{bmatrix} x_b \\ -y_a \\ -z_b \\ -z_b \end{bmatrix} \quad v_{13}^9 = \begin{bmatrix} x_b \\ -y_a \\ -z_b \\ -z_b \end{bmatrix} \quad v_{14}^9 = \begin{bmatrix} x_b \\ -y_a \\ -z_b \\ -z_b \end{bmatrix}$$

$$v_{21}^9 = \begin{bmatrix} x_a \\ -y_a \\ -z_b \\ z_b \end{bmatrix} \quad v_{22}^9 = \begin{bmatrix} x_a \\ -y_a \\ z_b \\ -z_b \end{bmatrix} \quad v_{23}^9 = \begin{bmatrix} x_a \\ -y_a \\ z_b \\ -z_b \end{bmatrix} \quad v_{24}^9 = \begin{bmatrix} x_a \\ -y_a \\ z_b \\ -z_b \end{bmatrix}$$

$$v_{31}^9 = \begin{bmatrix} x_a \\ -y_b \\ z_b \\ -z_b \end{bmatrix} \quad v_{32}^9 = \begin{bmatrix} x_a \\ -y_b \\ -z_b \\ z_b \end{bmatrix} \quad v_{33}^9 = \begin{bmatrix} x_a \\ -y_b \\ -z_b \\ z_b \end{bmatrix} \quad v_{34}^9 = \begin{bmatrix} x_a \\ -y_b \\ -z_b \\ z_b \end{bmatrix}$$

$$v_{41}^9 = \begin{bmatrix} x_b \\ -y_b \\ z_b \\ z_b \end{bmatrix} \quad v_{42}^9 = \begin{bmatrix} x_b \\ -y_b \\ z_b \\ z_b \end{bmatrix} \quad v_{43}^9 = \begin{bmatrix} x_b \\ -y_b \\ z_b \\ z_b \end{bmatrix} \quad v_{44}^9 = \begin{bmatrix} x_b \\ -y_b \\ z_b \\ z_b \end{bmatrix}$$

<u>Ellipsoid $\mathcal{E}_9$</u>

$$S_1 = \begin{bmatrix} 1.1459 & 0 & 0 & 0 \\ 0 & 1.1459 & 0 & 0 \\ 0 & 0 & 0.0050 & 0 \\ 0 & 0 & 0 & 0.0050 \end{bmatrix} \quad s_1 = \begin{bmatrix} -0.7 \\ 0.7 \\ 0 \\ 0 \end{bmatrix}$$

Biography

Born in Ratchaburi, Thailand, in 1987. Sompol Suntharasantic finished his high school, Phichit Pittayakom, in 2005 and passed the entrance examination to Chulalongkorn University. He obtained his Bachelor's Degree in Electrical Engineering in 2009. He was granted "Sitkonkuti" Scholarship from Electrical Enginnering Department to pursue his Master's degree in electrical engineering at Chulalongkorn University, Thailand, since 2009. He studied and did his research in Control Systems Research Laboratory.

Throughout the graduate studies, Sompol's research was under the supervision of Assistant Professor Manop Wongsaisuwan. His field of interest includes nonlinear control, piecewise-affine control, linear matrix inequalities, electronics, and robotics.

List of Publications

1. S. Suntharasantic, and M. Wongsaisuwan. Piecewise Affine Model and Control of Bicycle by Gyroscopic Stabilization. in *Proc. of ECTI-CON conference*. (2011): accepted for publication.

2. S. Suntharasantic, P. Rungtweesuk, and M. Wongsaisuwan. Piecewise Affine Model Approximation for Unmanned Bicycle. in *SICE Annual Conference*. (2011): paper submitted.